Stabilization of Energetic-Ion-Driven MHD Modes in the Advanced Helical Device, Heliotron J"

K. Nagasaki[1], S. Yamamoto[1], S. Kobayashi[1], Y. Nagae[2], K. Sakamoto[1], Y. I. Nakamura[2], T. Mizuuchi[1], H. Okada, [1], T. Minami[1], K. Masuda[1], S. Ohshima[1], S. Konoshima[1], N. Shi[1], Y. Nakamura[2], H. Y. Lee[2], L. Zang[2], S. Arai[2], H. Watada[2], M. Sha[2]、, H. Sugimoto[2], H. Fukushima[2], K. Hashimoto[2], N. Kenmochi[2], G. Motojima[3], Y. Yoshimura[3], K. Mukai[3], G. Weir[4], N. Marushchenko[5], F. Volpe[6], T. Estrada[7], F. Sano[1]

1 Institute of Advanced Energy, Kyoto University
2 Graduate School of Energy Science, Kyoto University[2]
3 National Institute for Fusion Science
3. University of Wisconsin-Madison, USA
5 Max-Planck Institute für Plasma Physik, Germany
6 Columbia University, USA
7 CIEMAT, Spain

Kyoto: Japan's "Heartland"

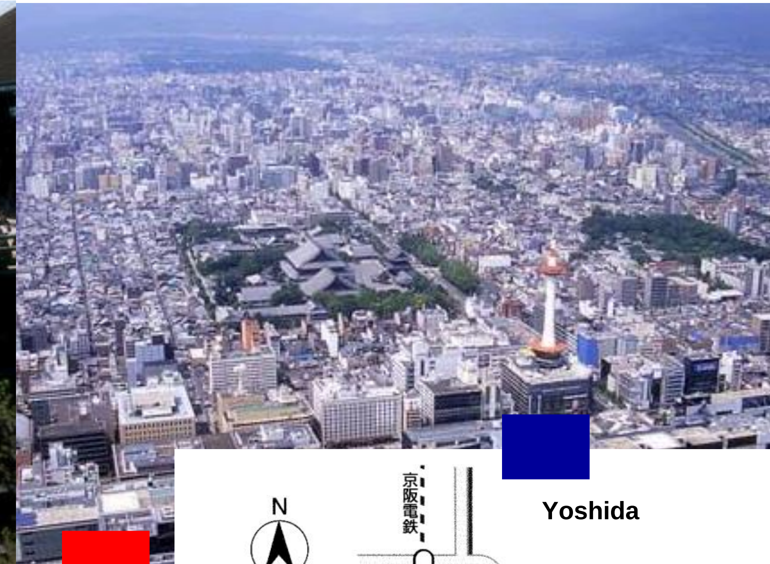

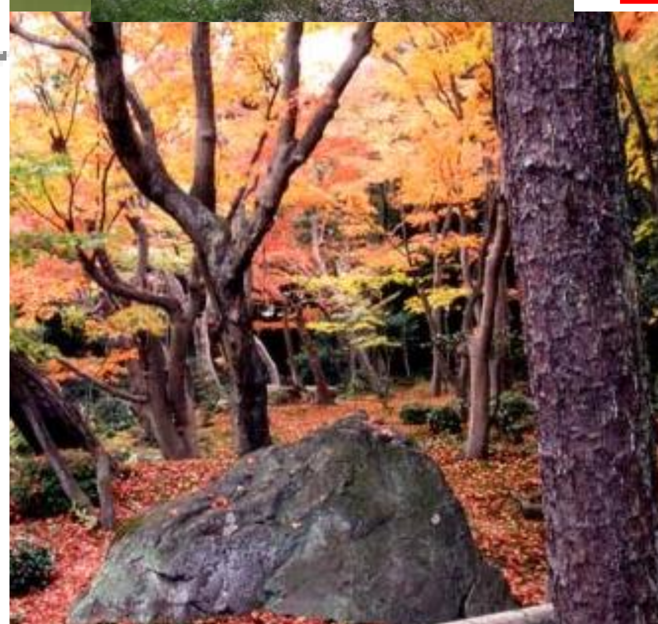

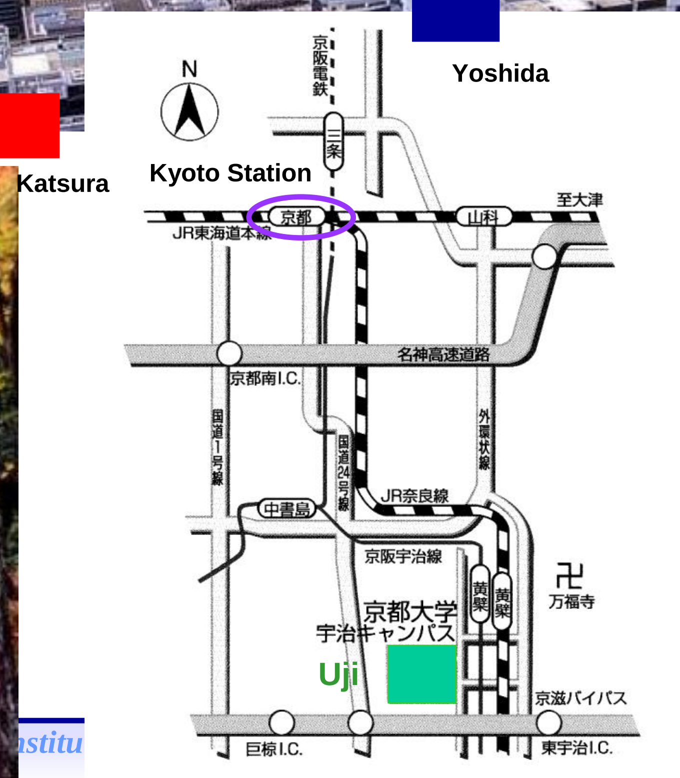

Kyoto University

As of May, 2013

Founded in 1897
Nobel Prize winners : 9 (Oct 2013)

Faculties : 10
Graduate schools : 16
Research institutes : 14
Research and educational centers : 18

Undergraduate student s: 13,585 (187)
Graduate students : 9,323 (1,212)
Foreign students : 1,399
Academic staffs : 2,787
Non-Academic staffs : 2,655

Scholastic exchange agreements :
94 Institutions of 34 countries

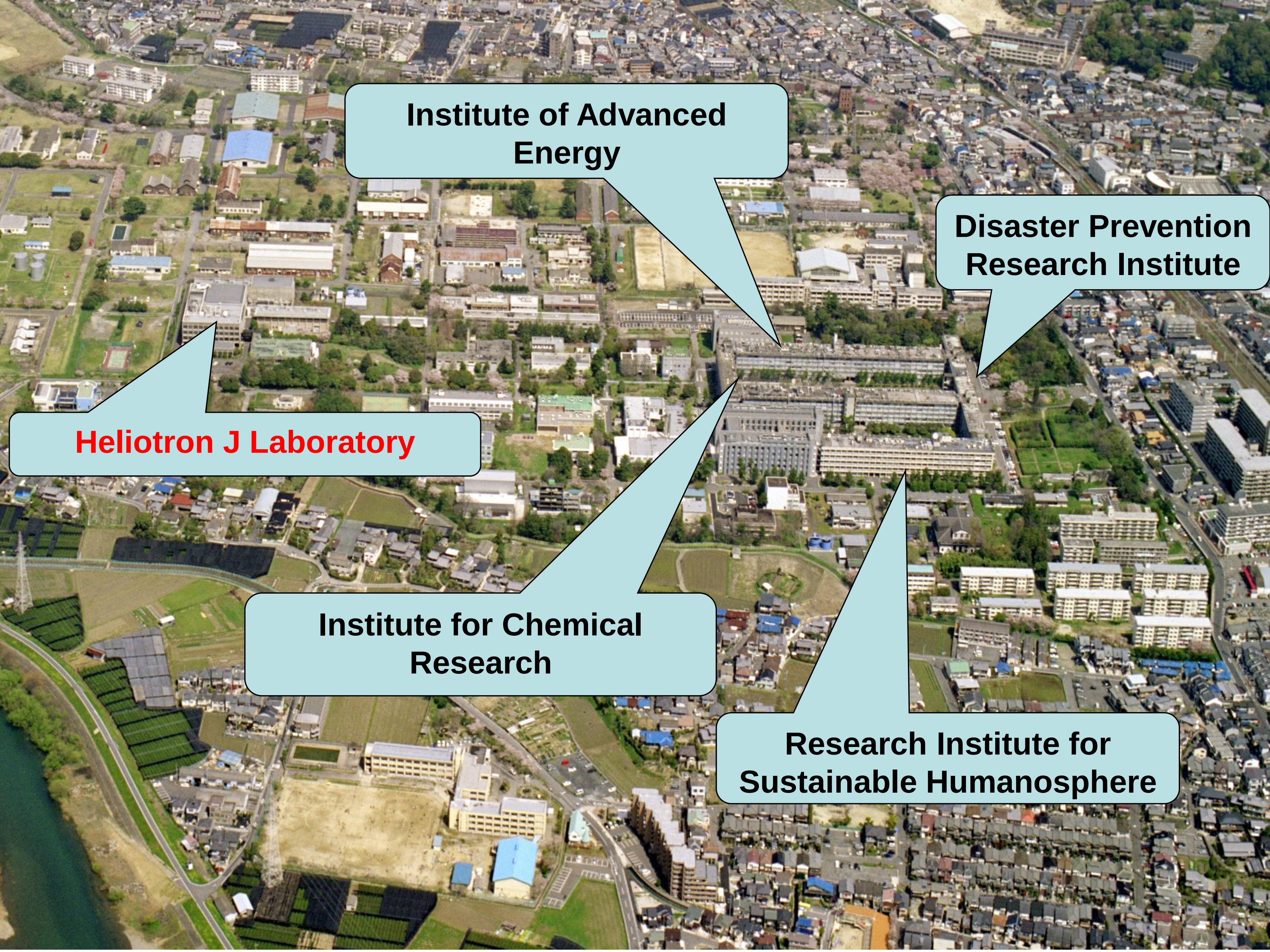
Institute of Advanced Energy
Disaster Prevention Research Institute
Heliotron J Laboratory
Institute for Chemical Research
Research Institute for Sustainable Humanosphere

Energy Research with Advanced Facilities

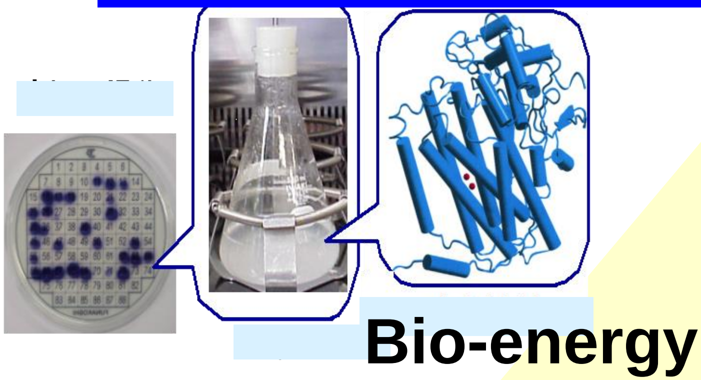

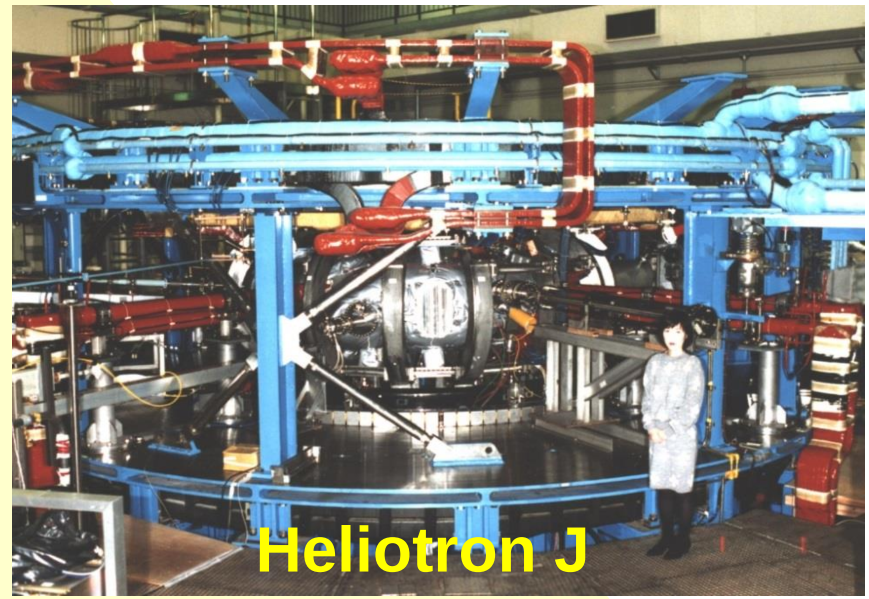

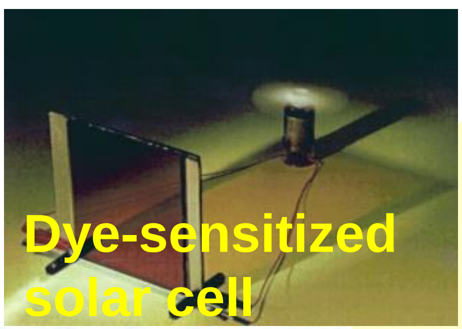

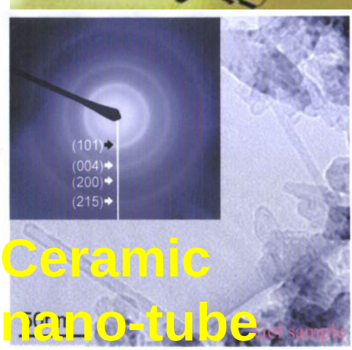

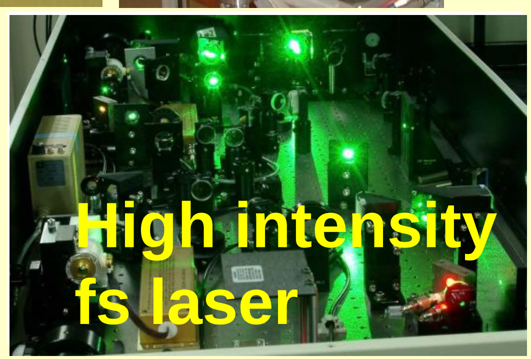

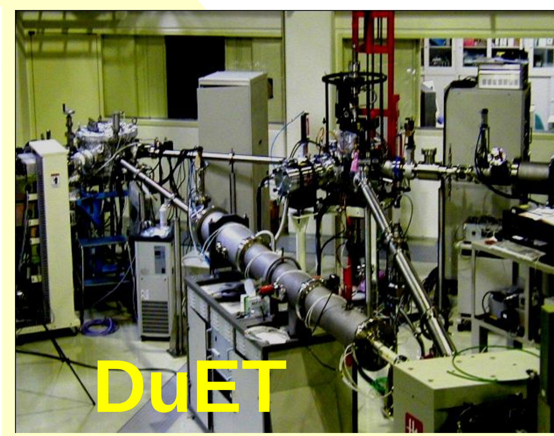

Outline

1. The Heliotron J Device and 70 GHz ECH/ECCD System
2. Energetic-particle-driven MHD modes
3. Modification of rotational transform profile by ECCD
3. Stabilization experiments of energetic-ion-driven MHD modes by ECCD
   - Stabilization of energetic particle modes by ECCD
   - Effect of magnetic shear
4. Conclusions

Heliotron J Project Aims To Develop Attractive Compact Fusion Reactor

FFHR

HSR

SPPS

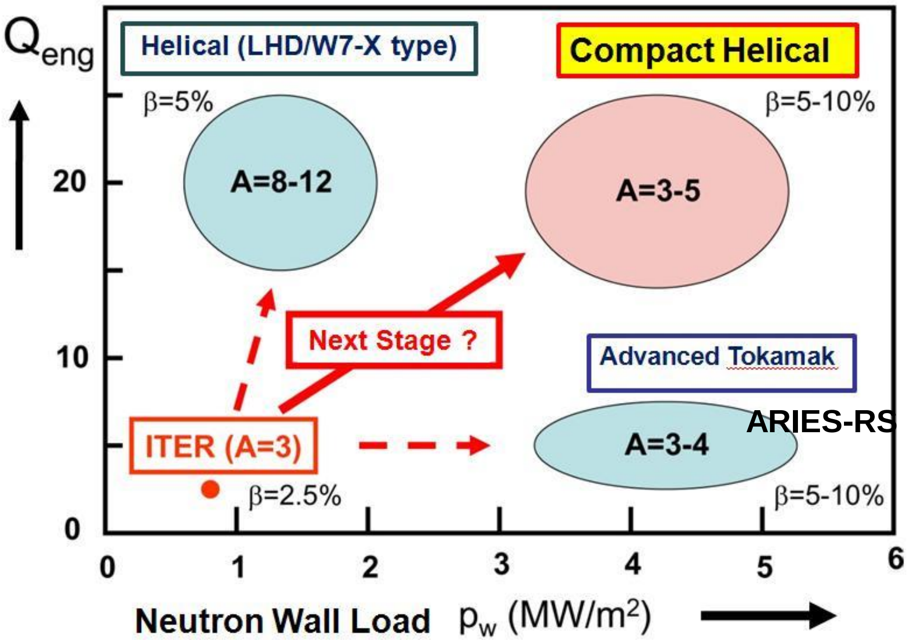

Compact Reactor

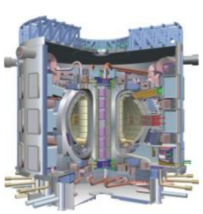

ITER

A steady-state, compact, high-β helical reactor

- No disruptions (currentless operation)
- No close conducting wall or active feedback control of instabilities
  - (no serious MHD instabilities)
- High Q_{eng} (= net $P_{ele.}$ / $P_{oper.}$) (at minimum recirculating powers)
- Wall loading (3~4 MW/m^2 under the development of advanced wall materials)

Planned/Operating Helical Systems

Plasma Device (Laboratory)	H-1 (ANU)	TJ-II (CIEMAT)	LHD (NIFS)	HSX (U. Wisconsin)	Heliotron J (Kyoto Univ.)	W7-X (MPI)
Schedule	1993~	1997~	1998~	1999~	1999~	2014~
Coil System	M=3 HFC+CR+TFC	M=4 HFC+CR+TFC	M=10 HFC+PFC	M=4 Modular Coil	M=4 HFC+TFC+PF C	M=5 SC Modular Coil
Major Radius Minor Radius Plasma Volume Magnetic Field Pulse Length	1.0 m 0.22 m 0.96 m^3 1.0 T 1 sec	1.5 m 0.1-0.25 m 1.43 m^3 1.5 T 0.5 sec	3.9 m 0.6-0.65 m 30 m^3 3 T CW	1.2 m 0.15 m 0.44 m^3 1.37 T 0.2 sec	1.2 m 0.18 m 0.82 m^3 1.5 T 0.5 sec	6.5 m 0.65 m 54 m^3 3.0 T > 10 sec
Heating System	ECH (0.2MW) Helicon (~ 0.5MW)	ECH (0.6MW) NBI (4MW)	ECH (3MW) ICH (3MW) NBI (32MW)	ECH (0.2MW)	ECH (0.5MW) NBI (1.5MW) ICH (2.5MW)	ECH, ICH NBI (20-30MW)
Features	Flexible configuration, High beta	High rotational transform, Low shear	Moderate shear	Quasi-helical symmetry	Local quasi-isodynamicity	Quasi-isodynamicity
Schematic View		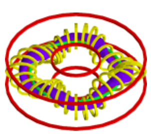	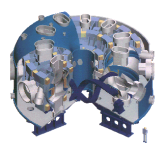	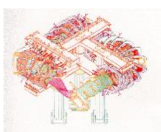	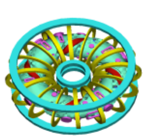	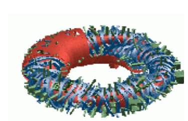

Heliotron J Device

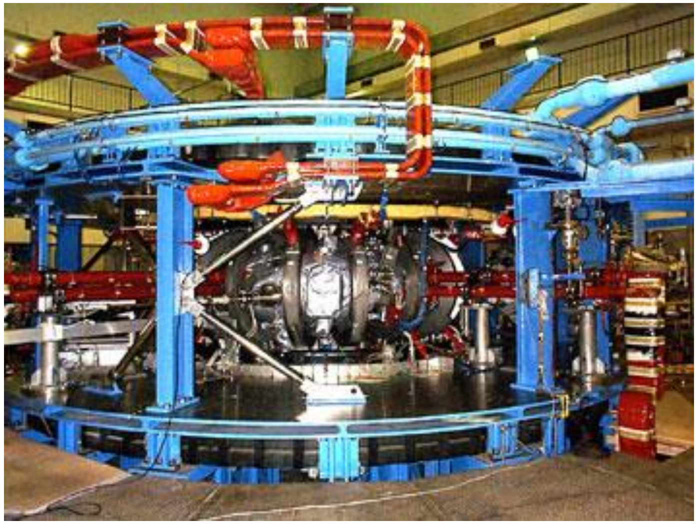

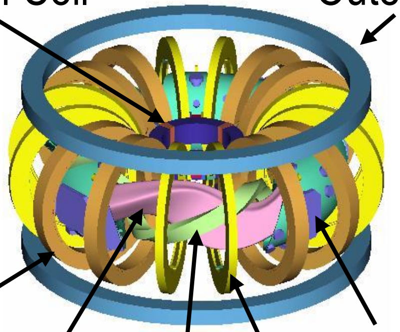

Major Radius: R=1.2 m
Plasma Minor Radius : a=0.1-0.2 m
Magnetic Field: B≦1.5 T
Vacuum iota: 0.3-0.8 with low magnetic shear
Heating System: ECH 0.4MW
NBI 0.8MW
ICRF 0.4MW
Magnetic coil system :
- one l/m=1/4 continuous helical coil
- two sets of toroidal coils
- three pairs of vertical field coils

Typical plasma parameters;

n_e=0.2-4 x 10^{19} m^{-3}

T_e=0.3-1 keV

T_i=150-200 eV

Top View of Heliotron J Device

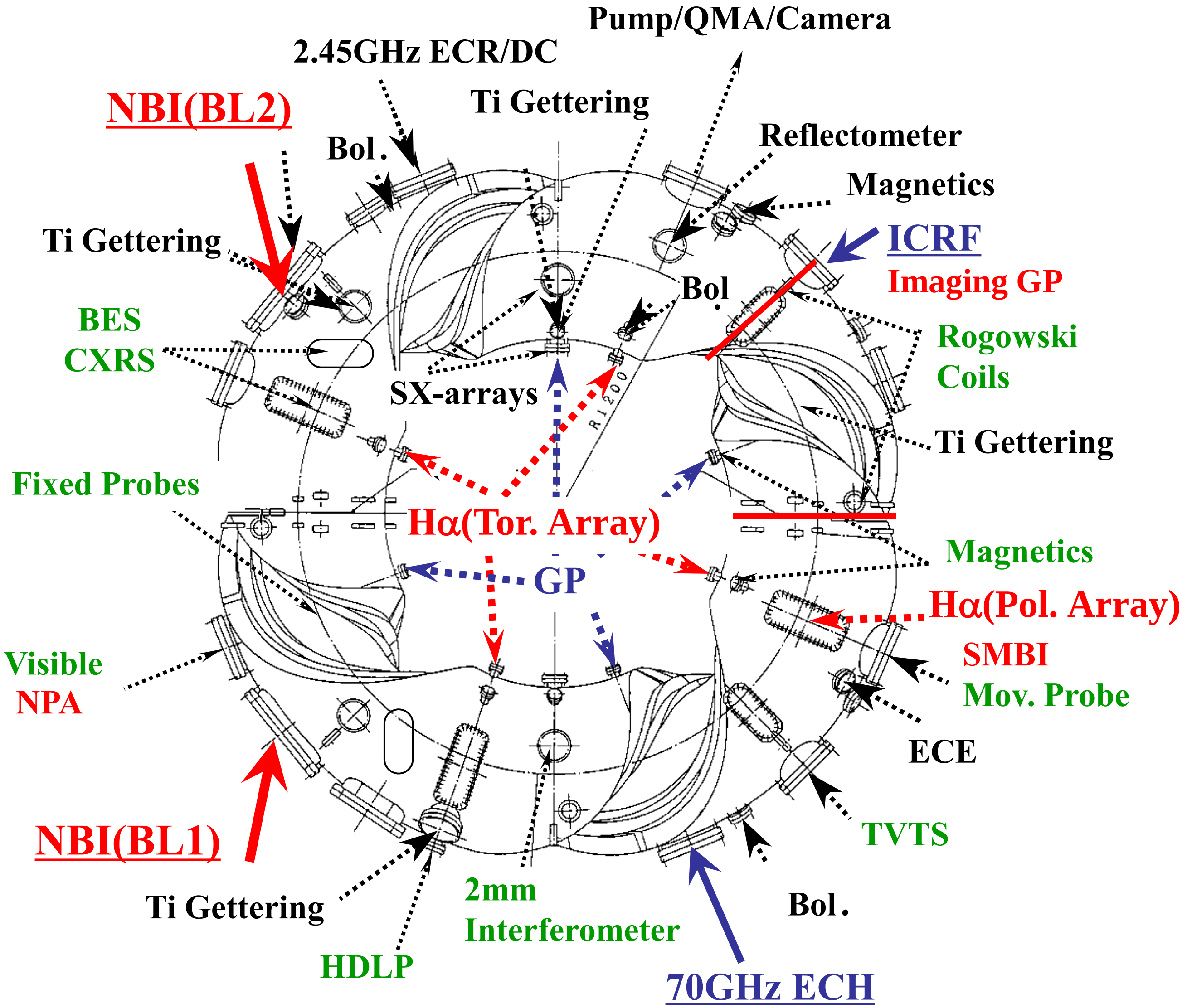

Magnetic Field Structure of Heliotron J

Magnetic flux surfaces

straight section

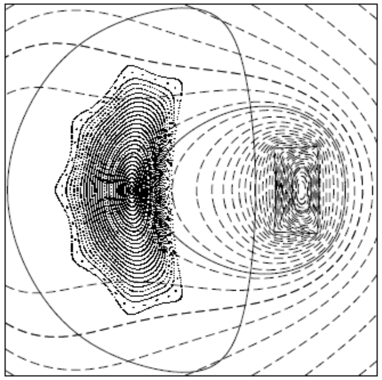

corner section

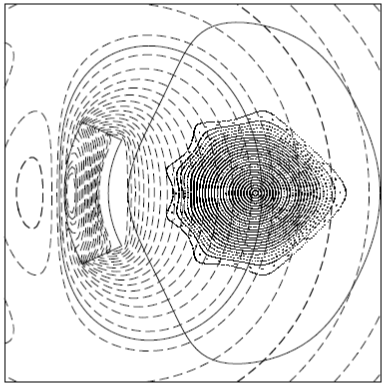

Rotational transform ι/2π

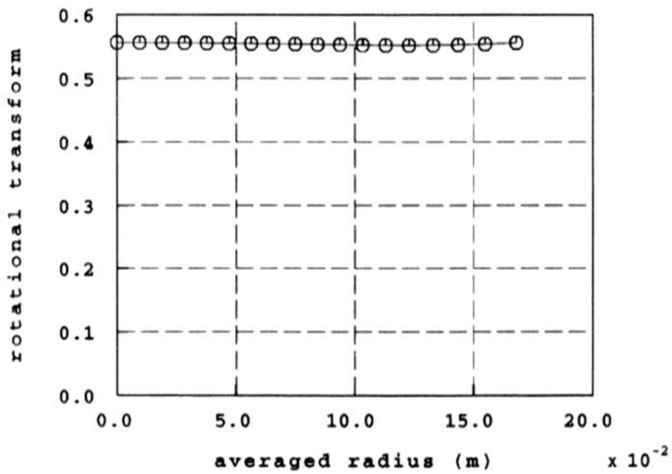

Magnetic field along axis

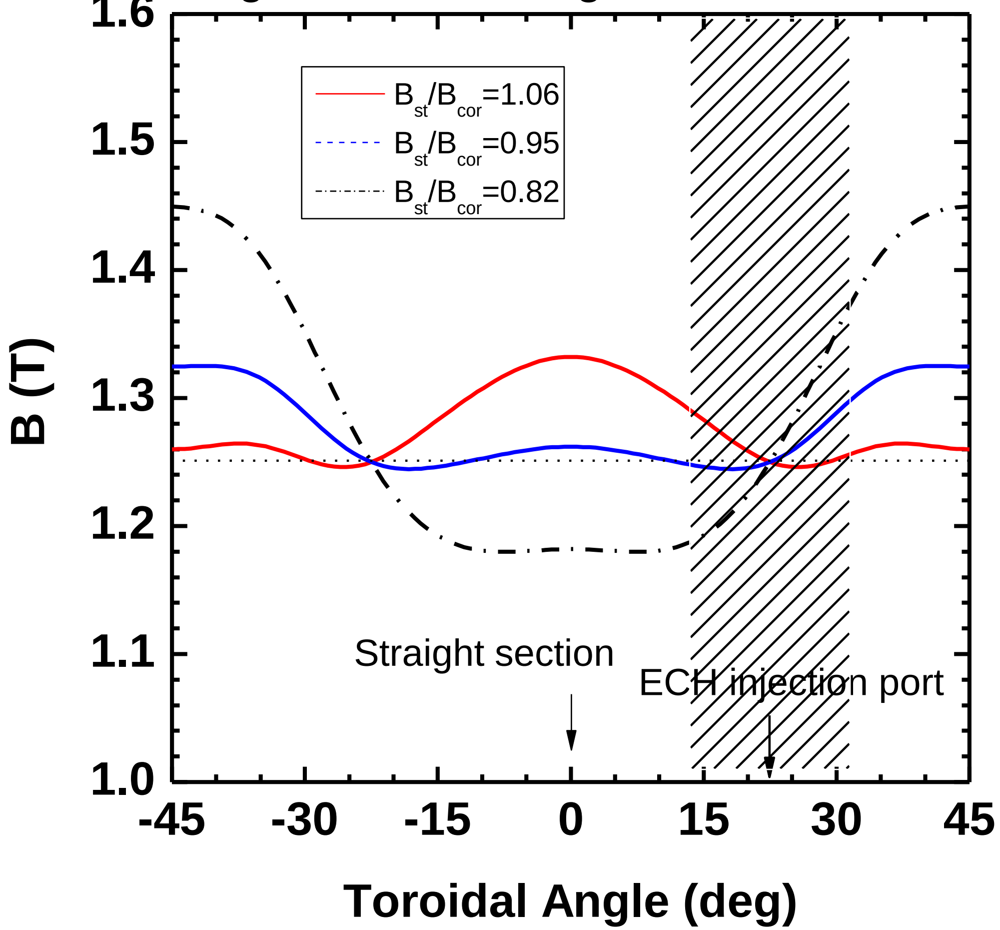

Shear Alfvén Waves

- Shear Alfvén Waves are transverse electromagnetic waves that propagate along the magnetic field
  - Dispersionless: $\omega = k_{||} v_A$
  - Alfven Speed: $v_A = B/(\mu_0 n_i m_i)^{1/2}$
  - $E_{||}$ is tiny for $\omega << \Omega_i$
  - Particles move with field line
  - All frequencies below Ω_i propagate
- The damping rate of shear Alfvén waves is very large at the Alfvén resonance due to Coulomb collision and Landau damping

"Contiuum damping"

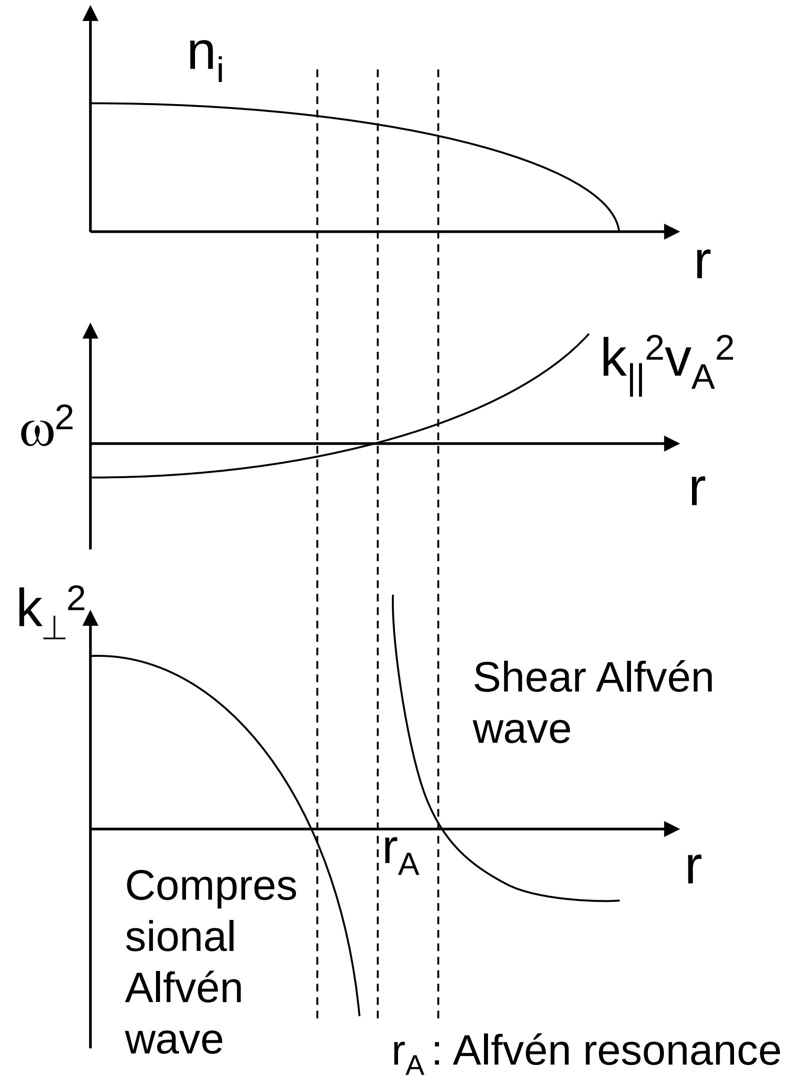

Global Alfvén Eigenmode (GAE)

- If $\omega^2 < k_{\|}^2 v_A^2$, the Alfvén resonance disappears, and the Shear Alfvén waves can propagate
- Since $-k_{\perp}^2$ is not so large, the eigenmodes is excited all over the plasma radius

“Global Alfvén Eigenmode (GAE)”

“Discrete Alfvén Eigenmode (DAE)”

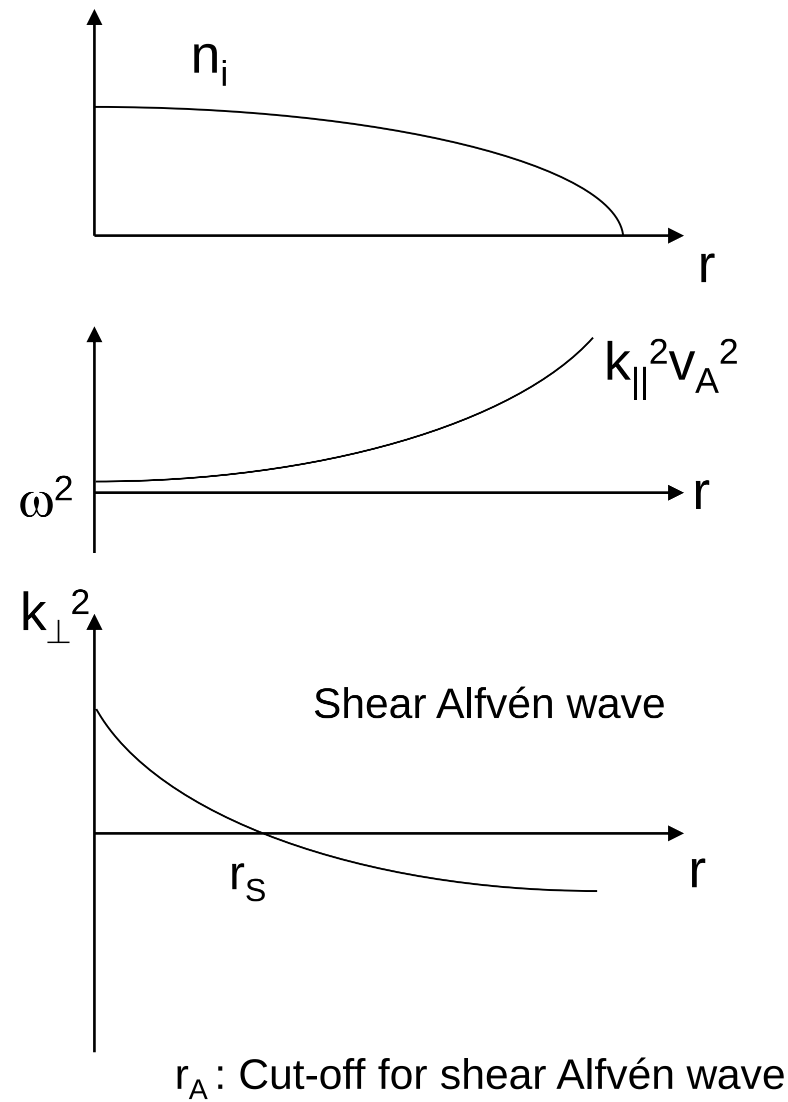

Shear Alfvén Continua in 2-D Magnetic Configuration

Profile of rotational transform (iota)

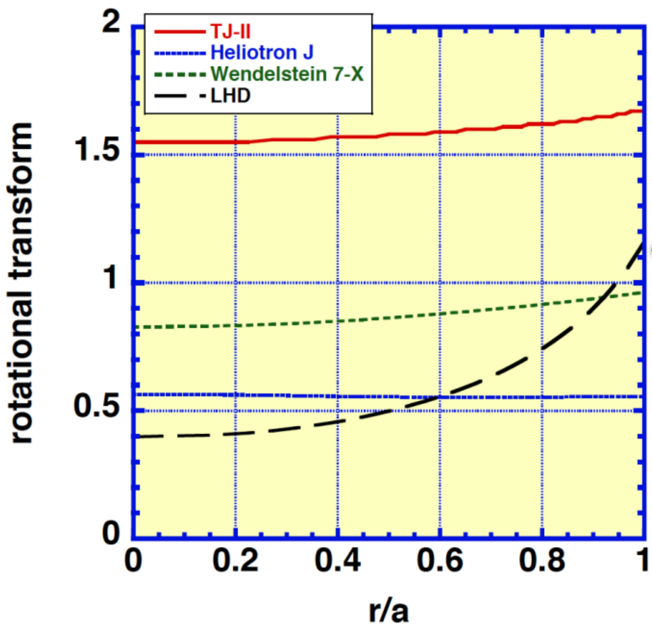

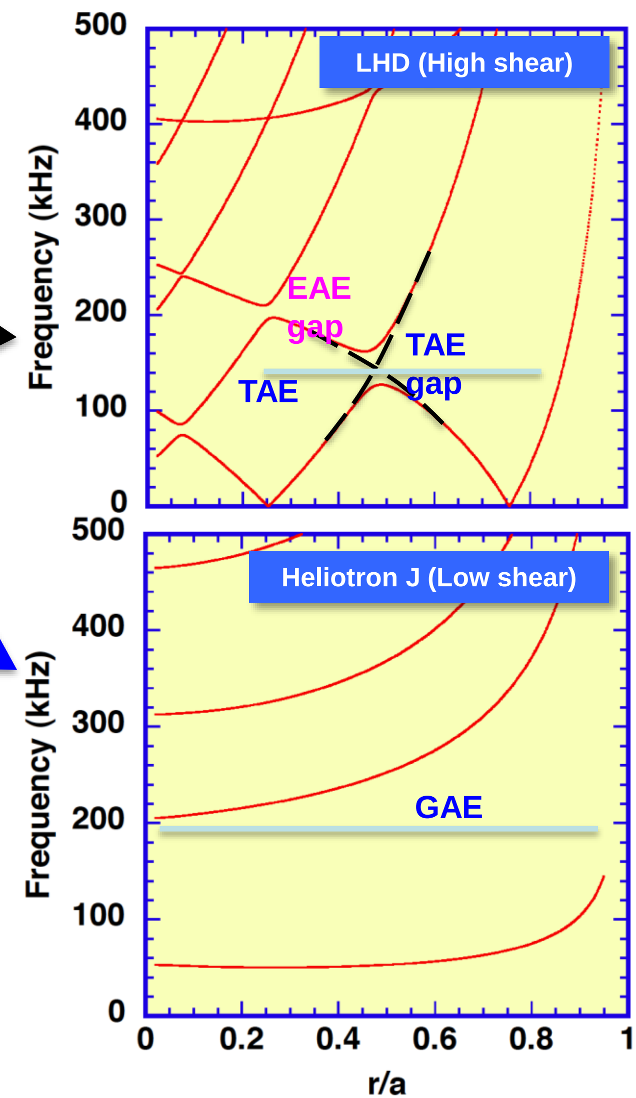

- ✓ In high magnetic shear configuration, shear Alfvén continua will intersect each other, then TAE and EAE gaps are formed.
- ✓ In low magnetic shear configuration, GAE can lie below and/or above the continuum instead of TAE (low-*n*).

Shear Alfvén Continua in 3-D Magnetic Configuration

✓ In Boozer coordinate, magnetic field strength is expressed as

$$|\mathbf{B}| = B_0\left[1+0.5\sum_{\mu\nu}\varepsilon_B^{\mu\nu}(\psi)\cos\left(\mu\theta-\nu N_p\phi\right)\right]$$

Mode coupling occurs between $(m, n) \Leftrightarrow (m\pm\mu, n\pm\nu N_p)$

$$\omega_* = \left|k_{\|*}^{\mu\nu}\right| v_{A*} \equiv \left|\mu\,\iota_* - \nu N_p\right|\frac{v_{A*}}{2R} \qquad \iota_* = \frac{2n+\nu N_p}{2m+\mu} \quad (\iota = 1/q)$$

(μ, ν) = (1,0): **TAE** / (2,0): **EAE** / (1,1): **$\mathbf{HAE_{11}}$** / (0,1): **$\mathbf{MAE_{01}}$**

Shear Alfvén continua (i/2p=0.56, N_f = 1)

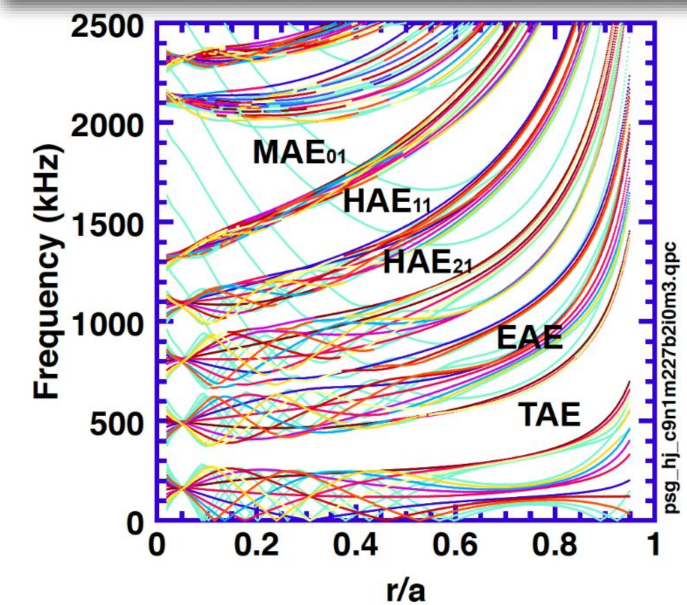

Iota dependence on AE gap (N_f=4)

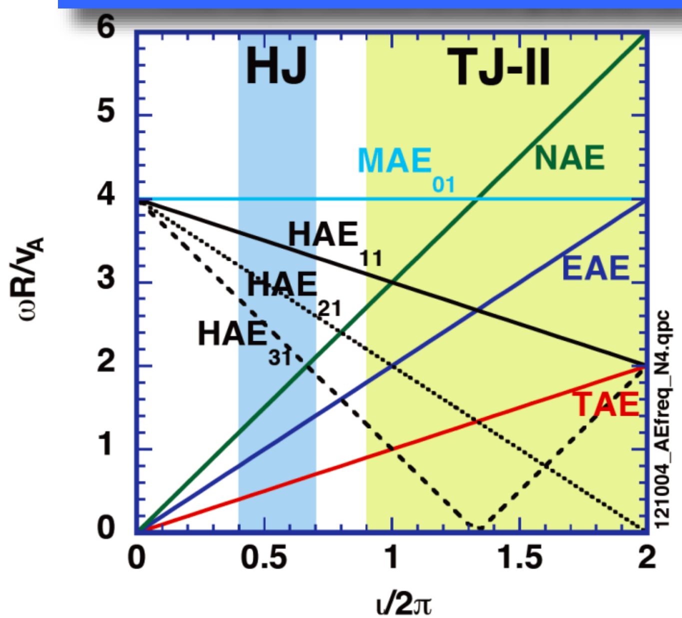

Energetic-Particle-Driven MHD Instabilities in Fusion Plasmas

- Energetic alpha particles are produced through deuterium-tritium fusion process and beam ions used for plasma heating
- They have a velocity comparable with the Alfvén velocity, can interact resonantly with shear Alfvén waves during slowing-down process
- Alfvén eigenmodes (AEs) are excited, resulting in enhanced radial transport of the energetic ions
- Even a small fraction of alpha power loss in a burning plasma can seriously damage plasma facing components

Energetic ion losses induced by TAE bursts in LHD.

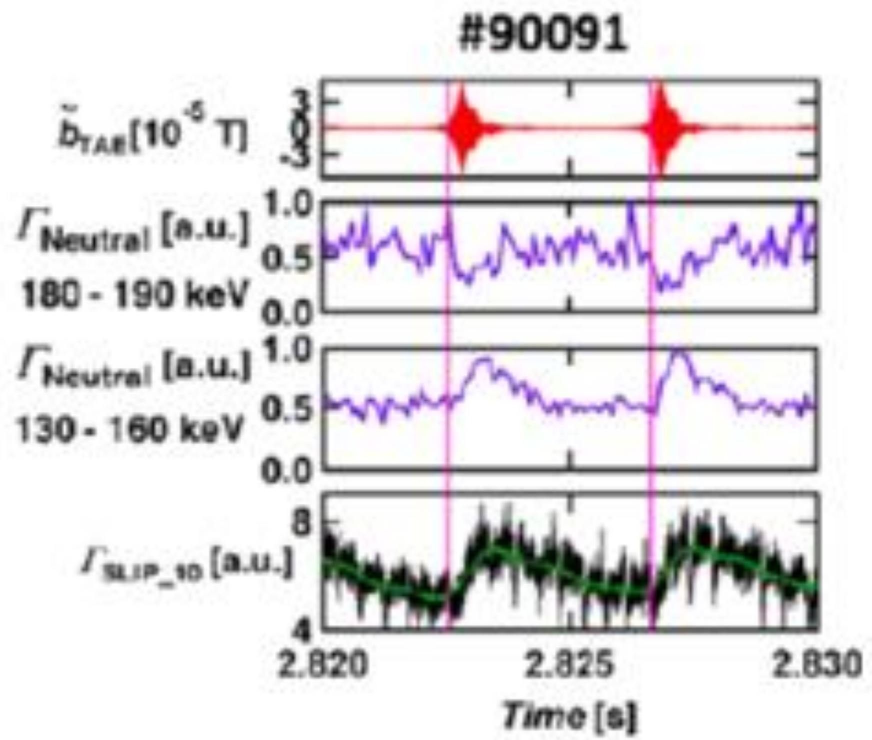

Ogawa, Nucl. Fusio (2010)

Observation of AEs in NBI-heated plasmas on Heliotron J

Typical waveform of AEs

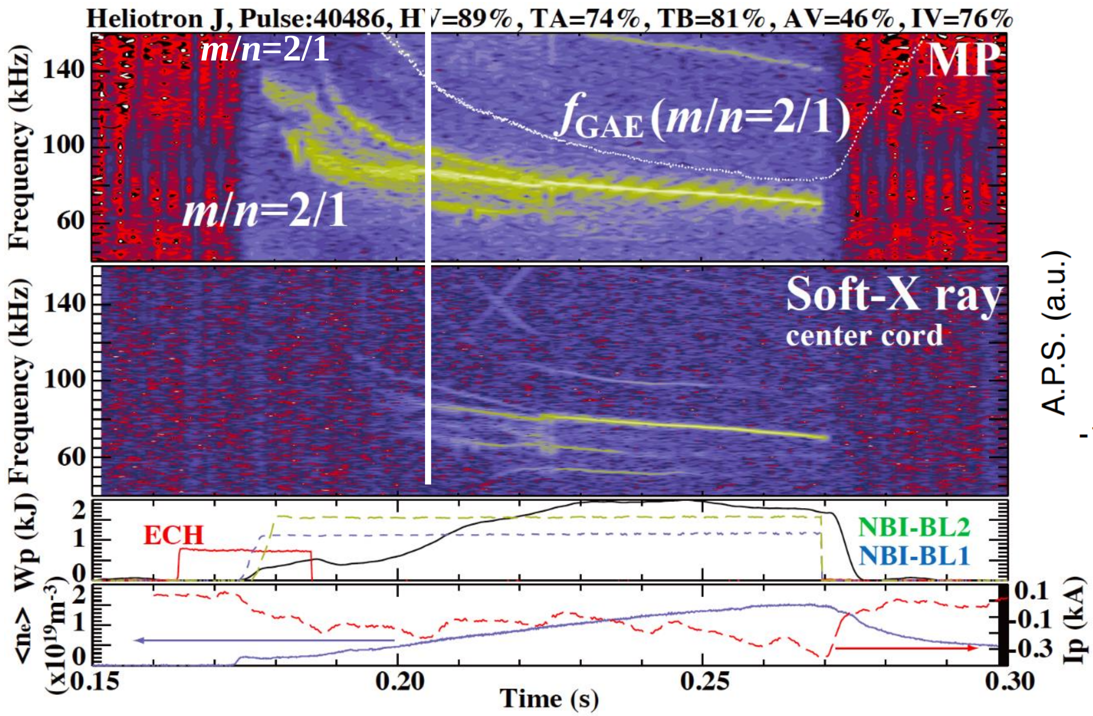

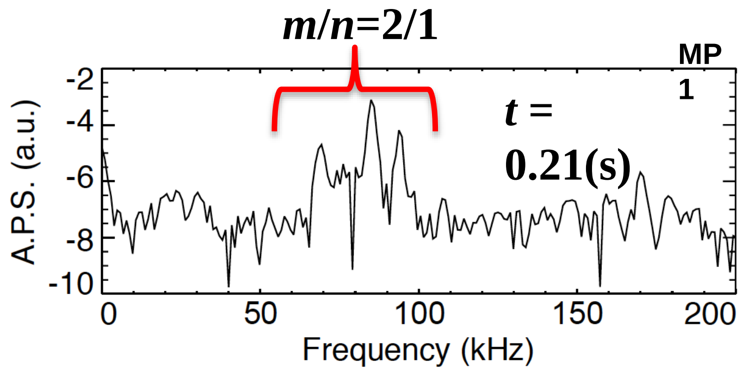

- In NBI heated plasmas, some coherent MHD instabilities are observed in the range of Alfvén frequency
- The frequencies are similar to those of the GAEs with *m*=2/*n*=1 (without impurity effect)

Identification of the mode as GAE

☆ Continua and eignmode are calculated by STELLGAP and AE3D coded by D. Spong

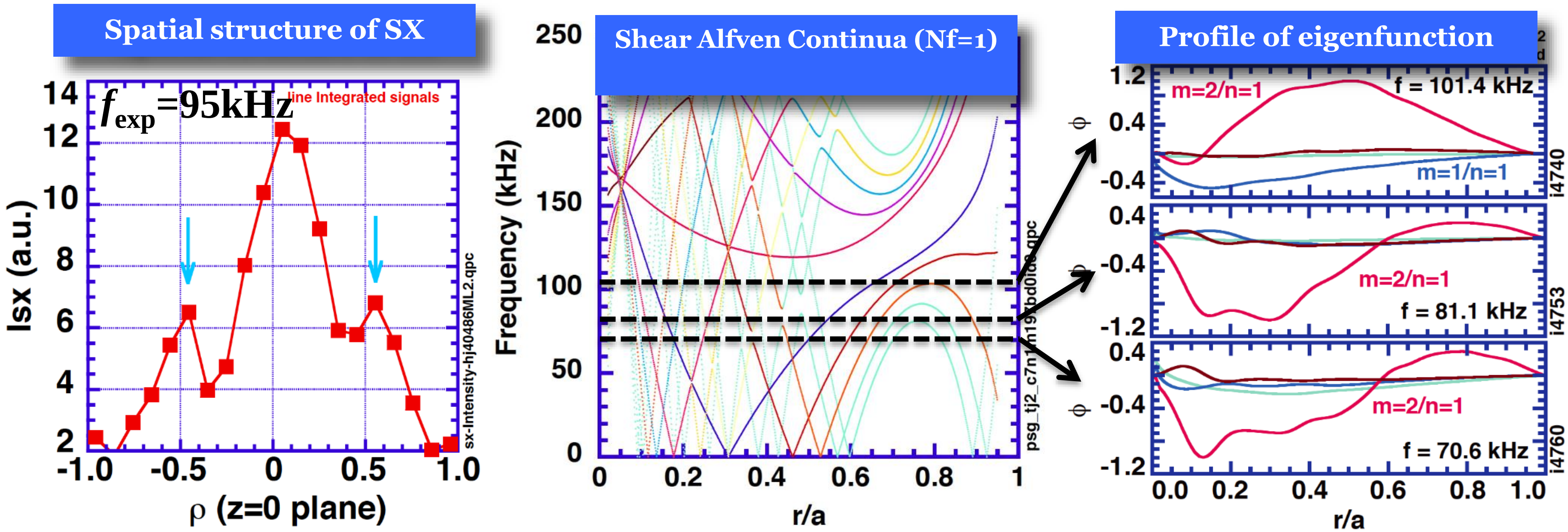

- The spatial structure of eigenmode with f_{cal} = 101 kHz agrees with that of the observed mode with f_{exp} = 95 kHz
- Comparison of experimental result with shear Alfvén spectra indicates that the observed modes are GAEs
- Effect of toroidal mode coupling on low-*n* GAE with N_f = 4 is weak

Energetic Particle Modes (EPM)

- Energetic particle modes (EPM) are excited when pressure of energetic particles (EP) is comparable to bulk pressure
- Energetic particles create a new wave branch
- Energetic particles resonate with mode, altering Im(ω)
- Intense drive overcomes continuum damping

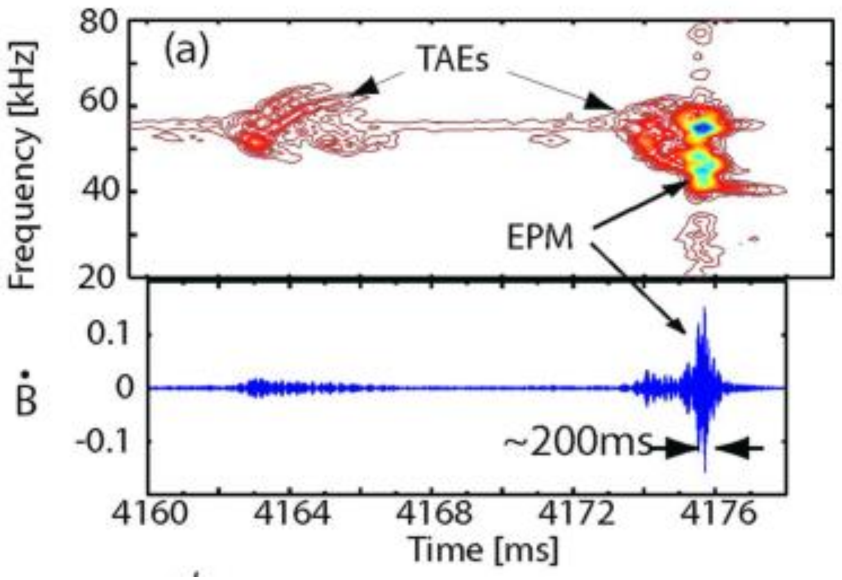

Shinohara, Nucl. Fusion (2001)

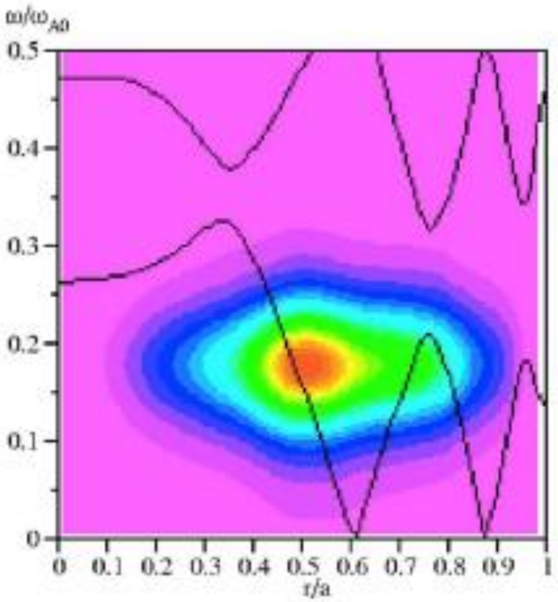

Briguglio, PoP (2007)

Observation of EPM

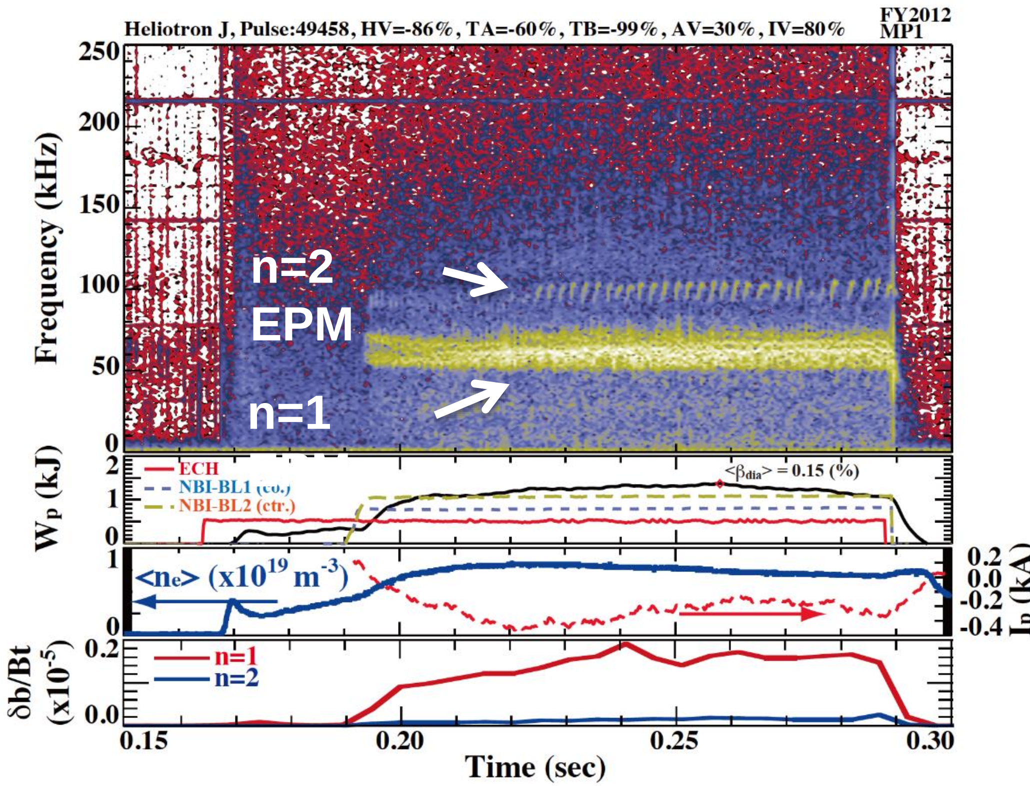

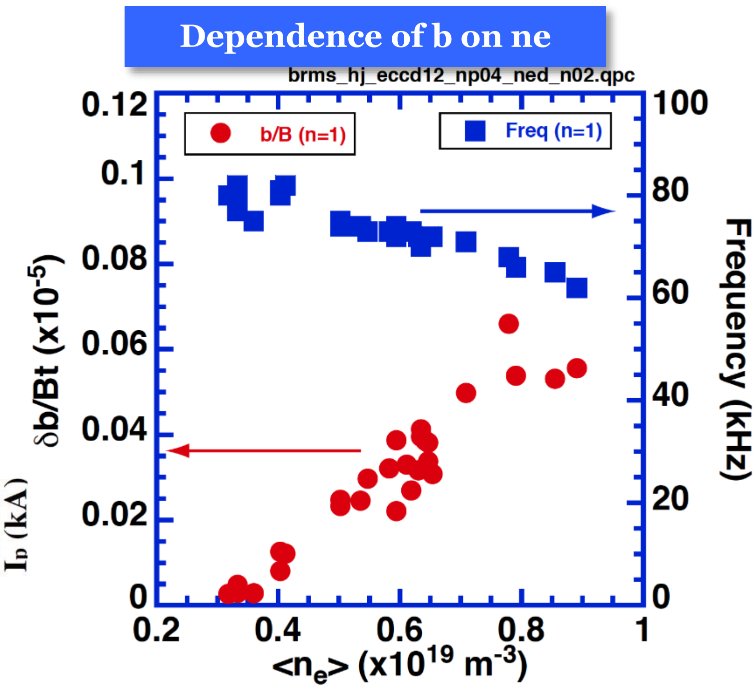

- The ratio of beam velocity to Alfven velocity is about 0.3.
- Observed mode frequency is not proportional to $n_e^{-0.5}$
- Mode amplitude depends on electron density

A Severe Impact of ECH on the AE Behavior Was Observed in DIII-D and TJ-II

- In DIII-D, ECH near q_{min} suppresses RSAE and lower amplitude TAEs are unstable in DIII-D
- In TJ-II, ECH+NBI causes steady frequency Aes to decrease in amplitude and begin chirping

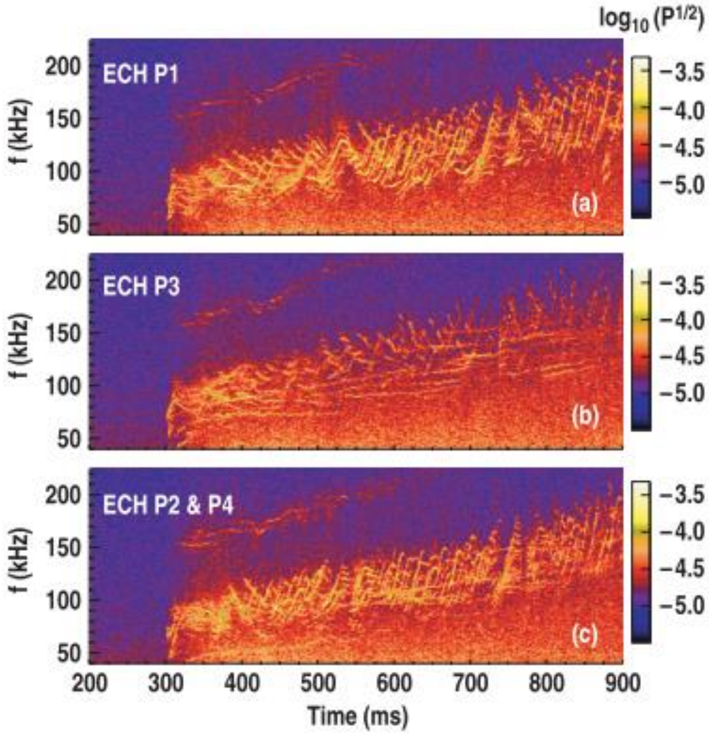

Van Zeeland, PPCF (2008)
Van Zeeland, Nucl. Fusion (2009)

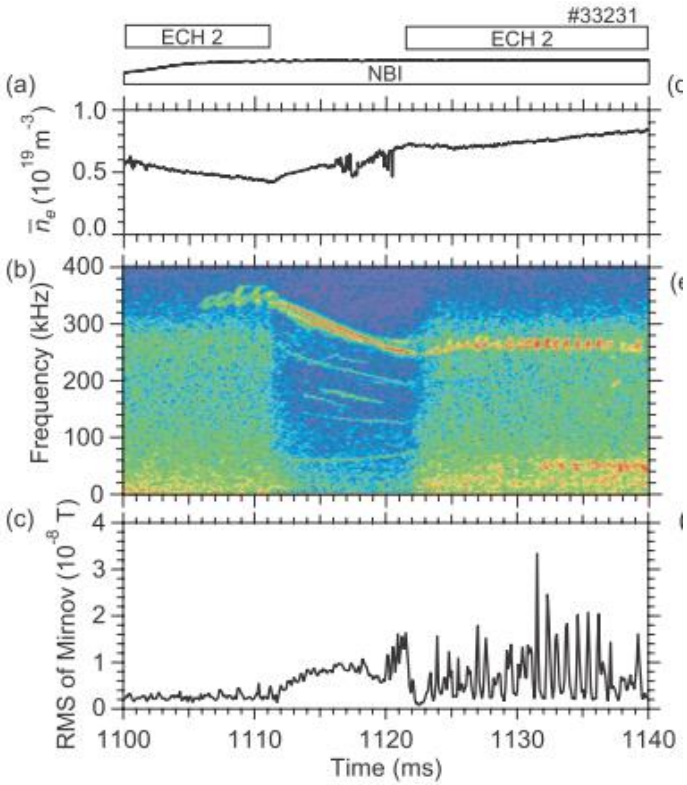

Nagaoka, Nucl. Fusion (2013)

70GHz ECH/ECCD System for Heliotron J

Gyrotron (0.5MW, 0.2sec)

Transmission line using corrugated W.G.

Polarizer

Power monitor

Launcher

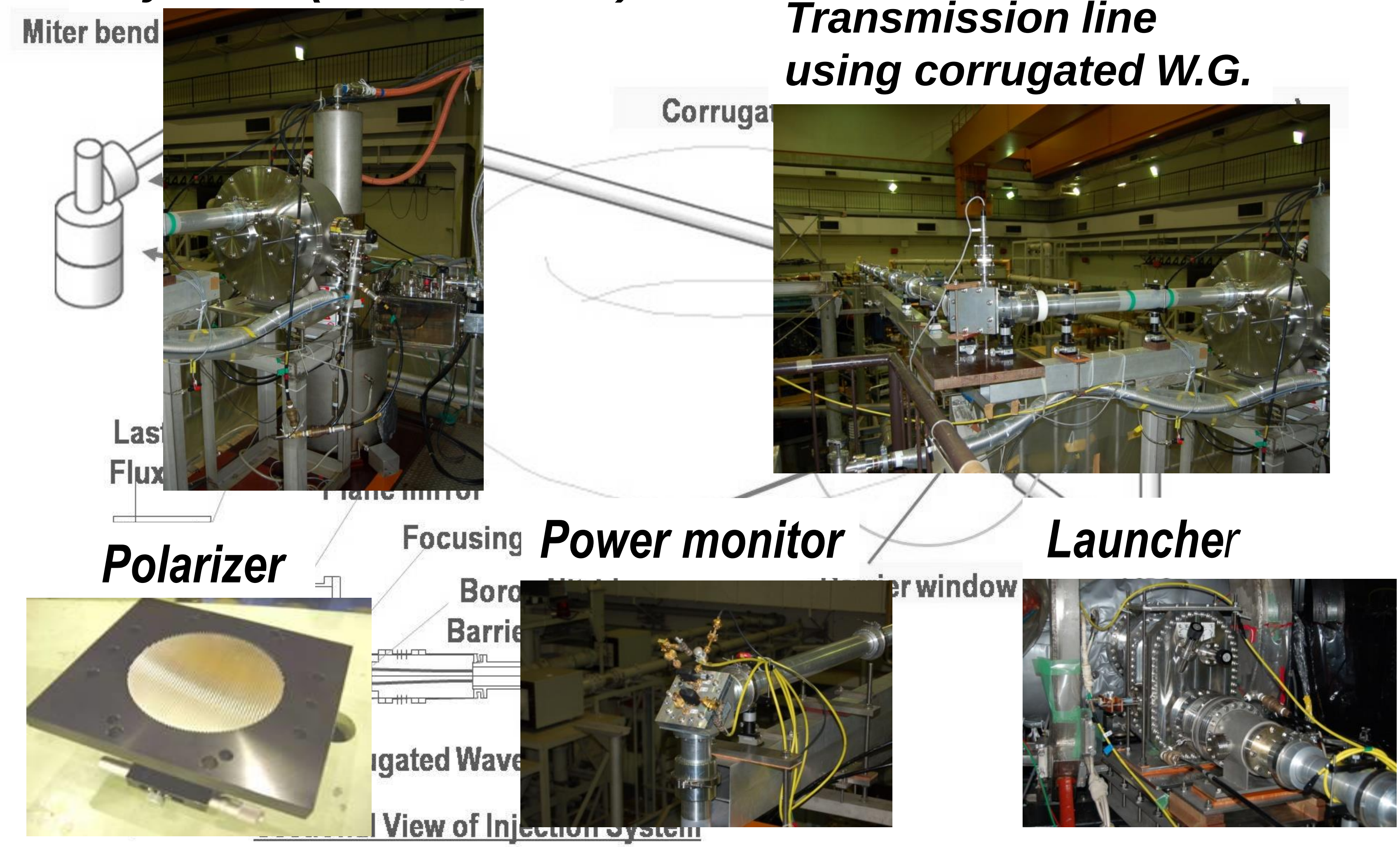

70GHz ECH/ECCD Launcher System

- A launching system with a focusing mirror and a steering mirror has been installed and operated in Heliotron J since the 2009 experimental campaign

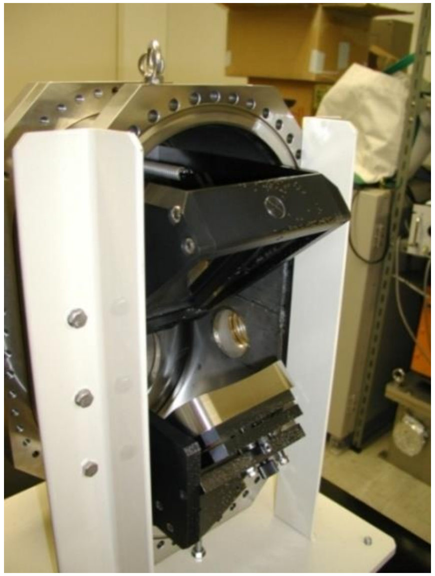

- Maximum injection power: P_{EC}=0.4MW
- Focused Gaussian beam, w=30 mm
- $|N_{||}| < +0.6$
- Possible to inject along magnetic axis

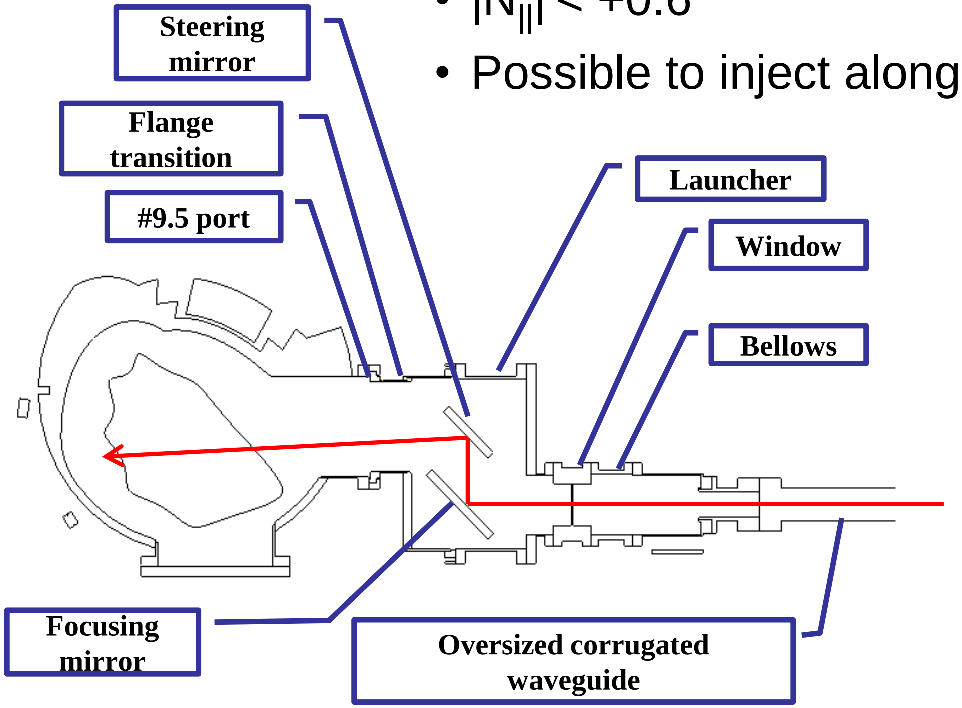

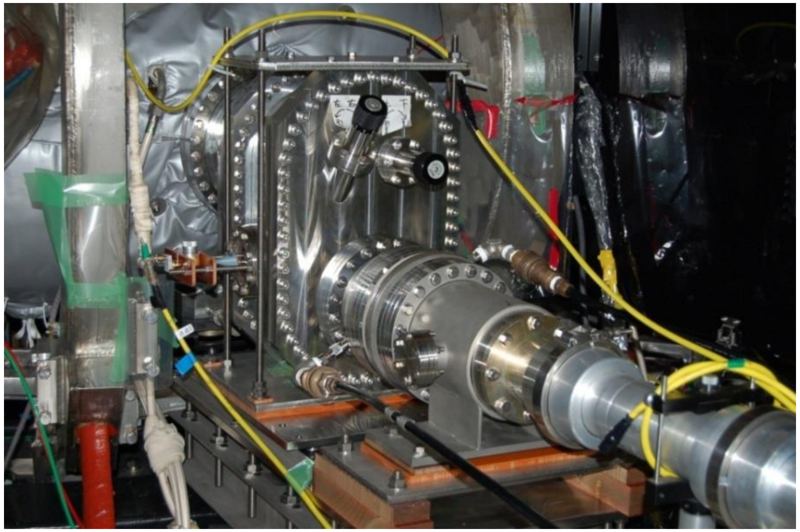

Second Harmonic X-mode ECCD

- The CD efficiency is calculated by applying the adjoint approach with parallel momentum conservation
- Good agreement was found between experimental results and TRAVIS code results in ECH-only plasmas

ECCD in ECH-only plasmas

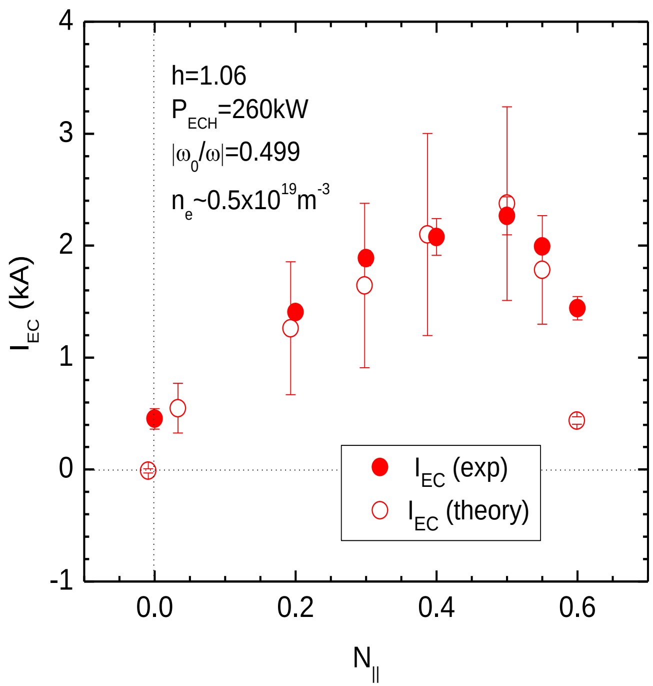

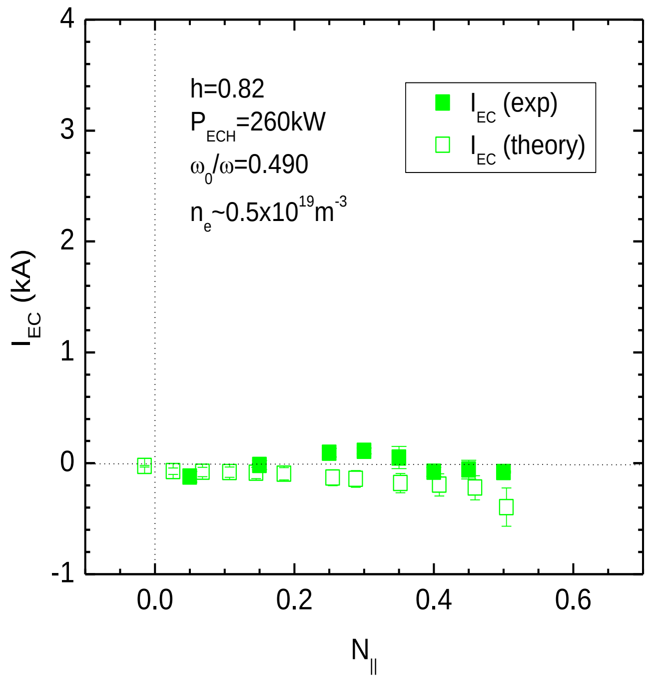

K .Nagasaki, Nucl. Fusion 51 (2011) 103035

ECCD Depends on Magnetic Field Structure

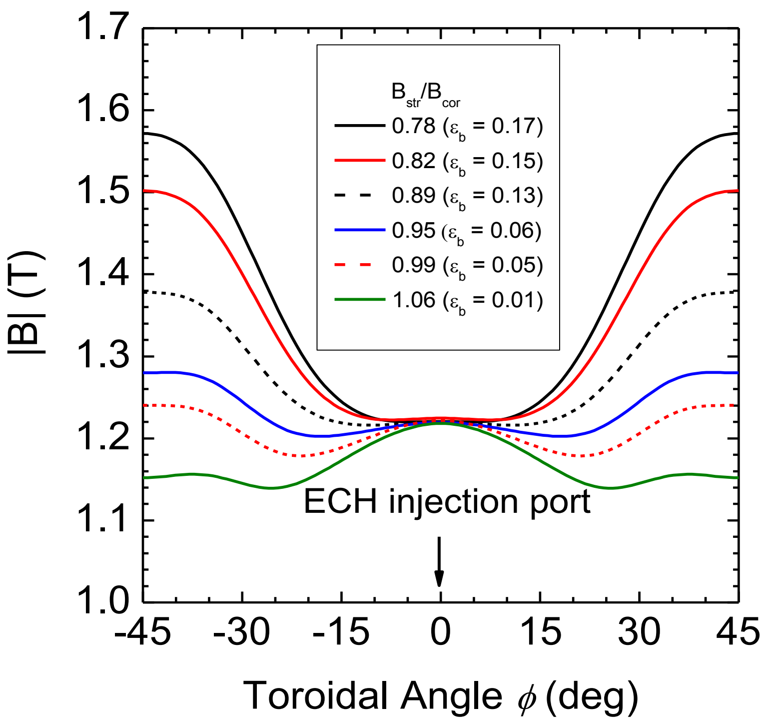

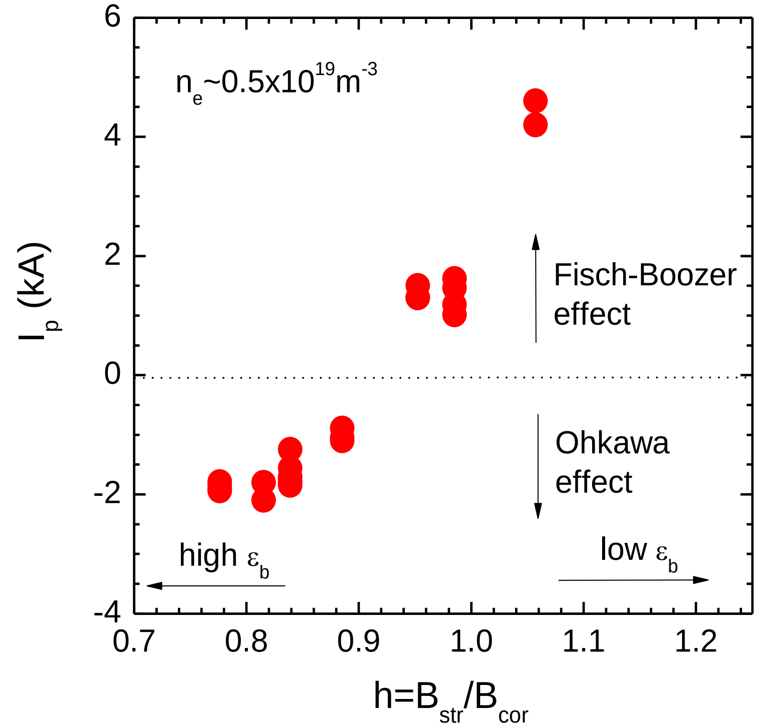

- The bumpiness control changes the magnetic ripple structure
- The toroidal current changes its flowing direction, depending on the ripple structure
- The current direction is explained by the balance between the Fisch-Boozer effect and the Ohkawa effect

K. Nagasaki, Nucl. Fusion (2010)

EC Current Modifies Rotational Transform Profile, Forming a Strong Magnetic Shear in Core Region

- The TRAVIS code predicts that the total current flows 2.9 kA at $N_{||}$ = 0.4, n_e=0.5×10^{19} m^{-3} and $T_e(0)$=0.8 keV

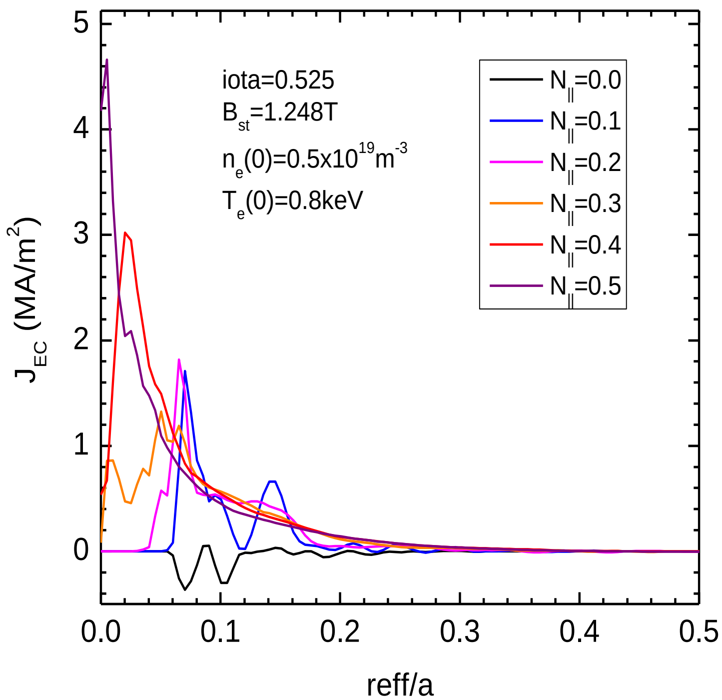

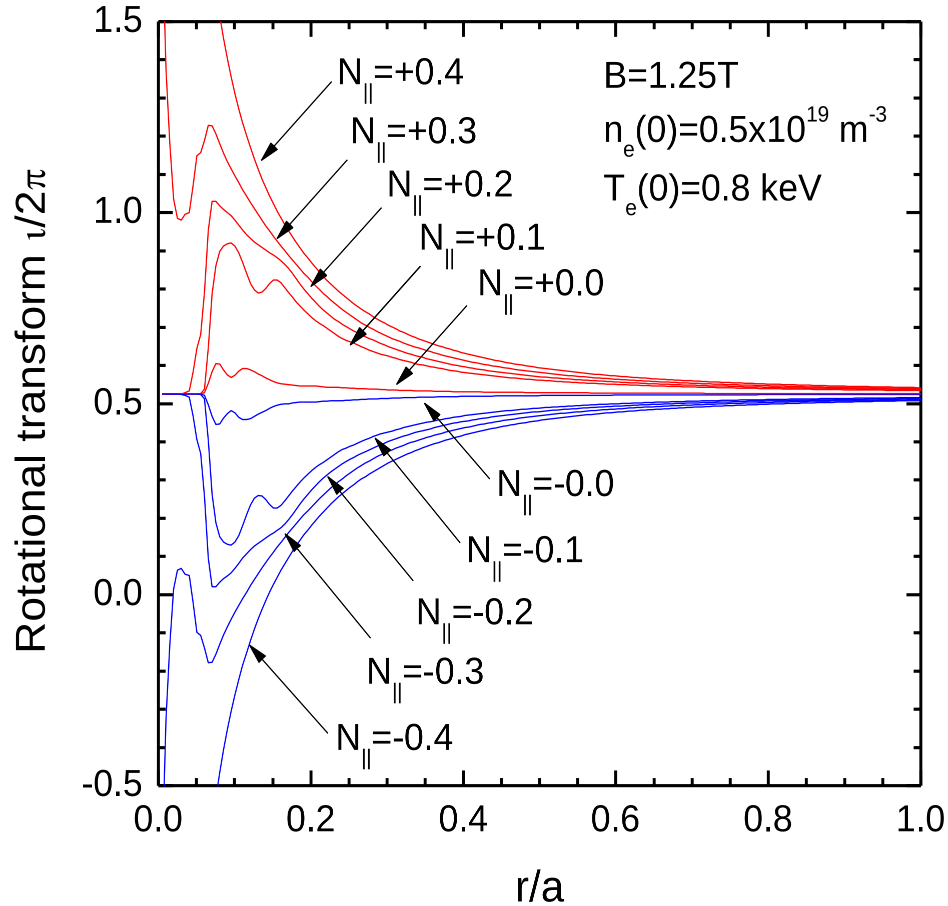

An Energetic-Ion-Driven MHD Mode Has Been Stabilized by Counter-ECCD

No ECCD ($N_{||}$=0.0)

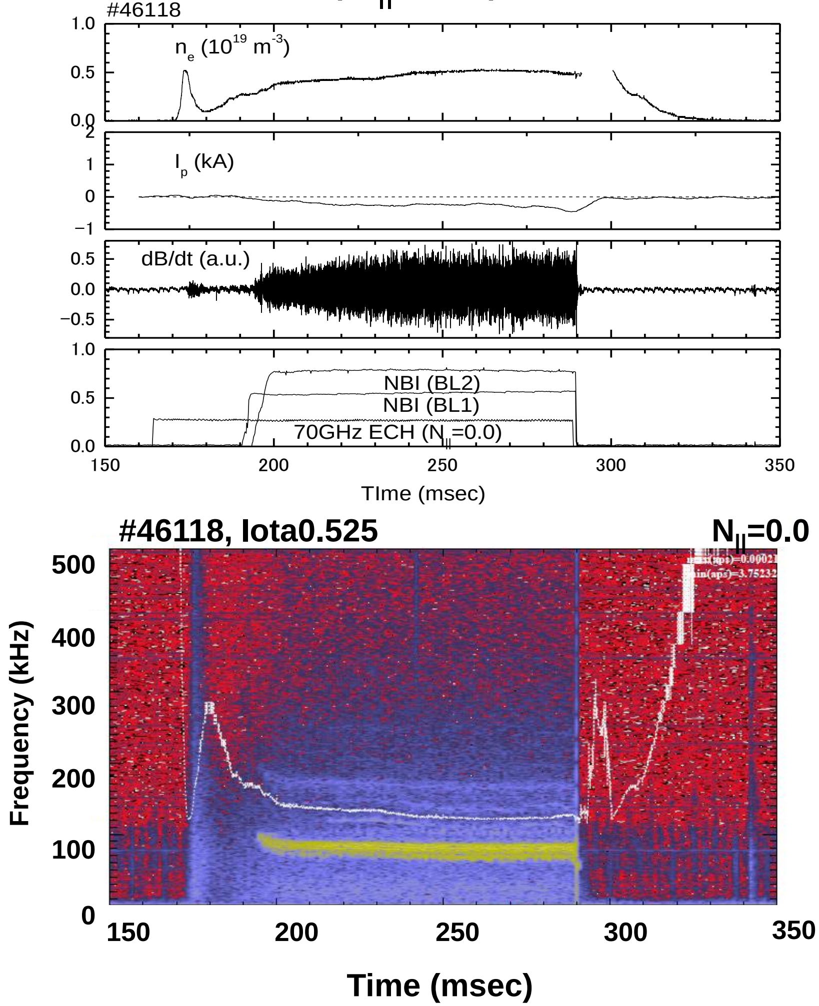

Counter-ECCD ($N_{||}$=-0.3)

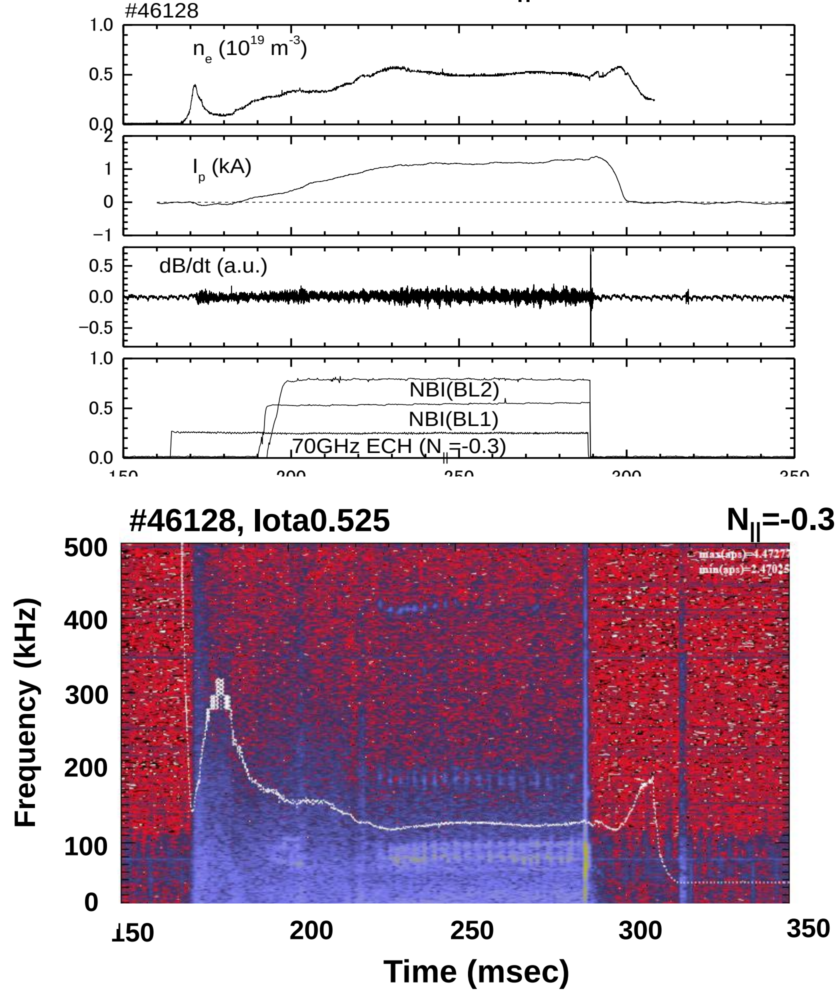

K .Nagasaki, Nucl Fusion 2013

The Observed Mode Appears to be Energetic Particle Mode

- Density fluctuation measurement using a Beam Emission Spectroscopy (BES) reveals that the mode of 80 kHz is localized at *r*/*a* ~ 0.6
- FFT analysis of Mirnov coil signals shows that the mode number is m/n = 4/2, rotating in the ion diamagnetic direction
- This mode has high coherence with magnetic probe signals, weak n_e dependence

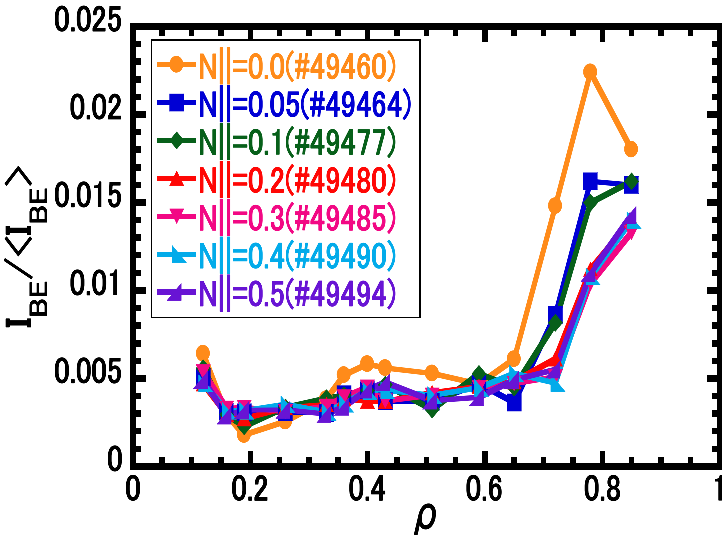

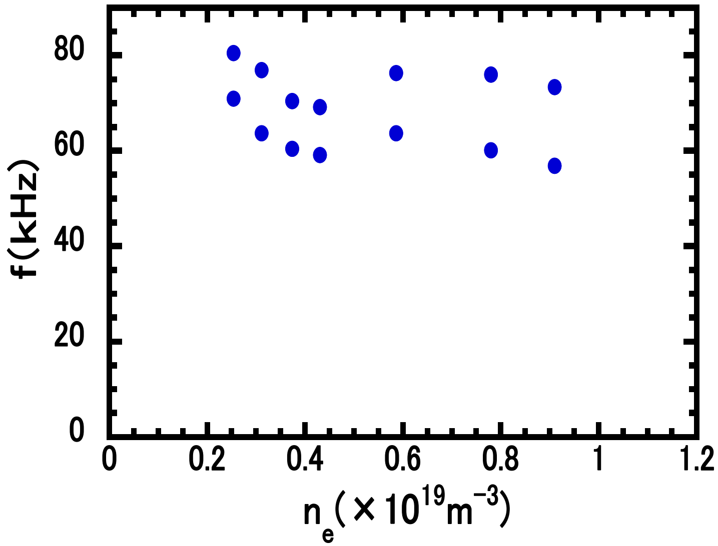

Radial Shift of EPM due to ECCD

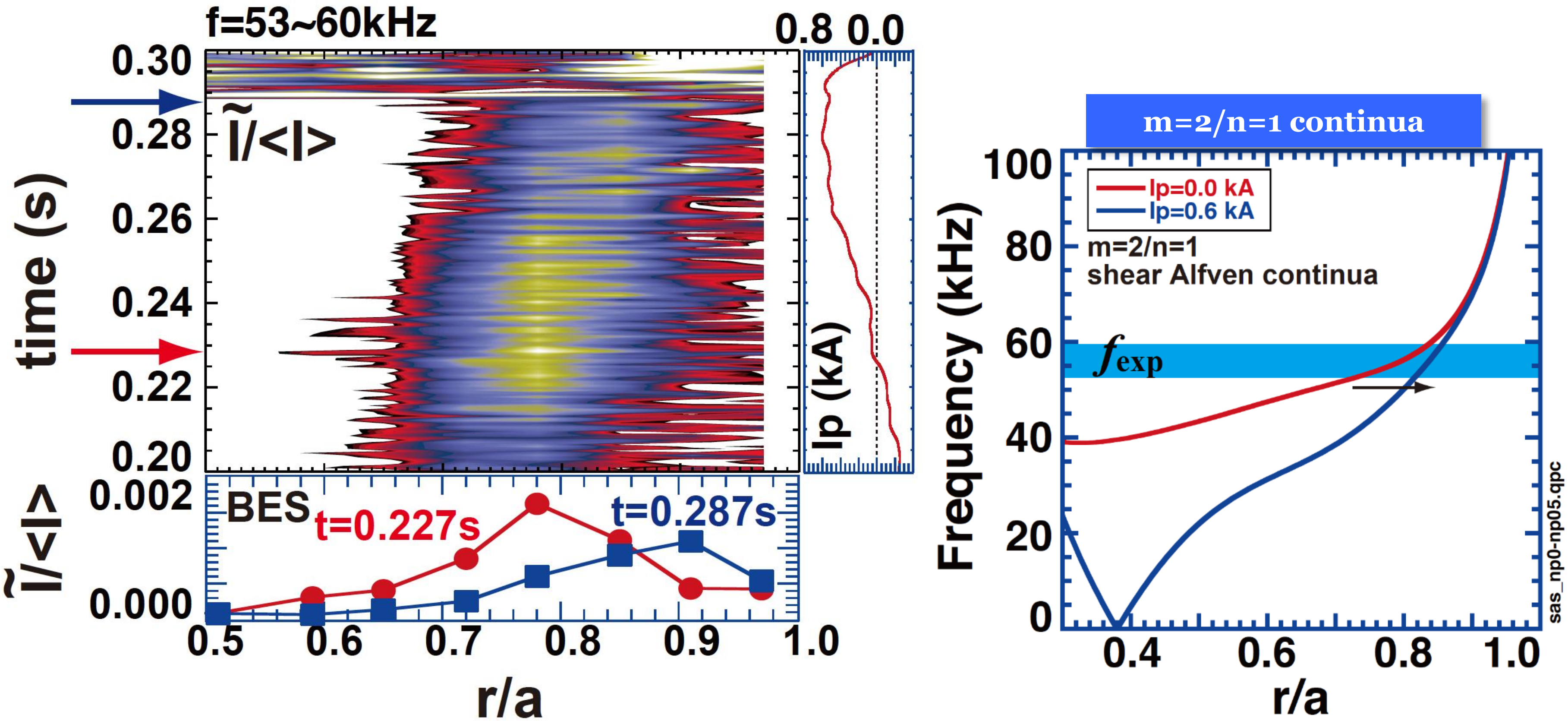

- ✓ Outward movement of EPM with n=1 during the ramp-up phase of plasma current is observed in BES measurements ($\tilde{n}_e/\langle n_e \rangle$).
- ✓ The movement can be explained by the change of shear Alfvén continuum due to the increasing of plasma current.

Amplitude of EPM Is Reduced As EC Driven current Evolves

- The mode suppression has no transition property

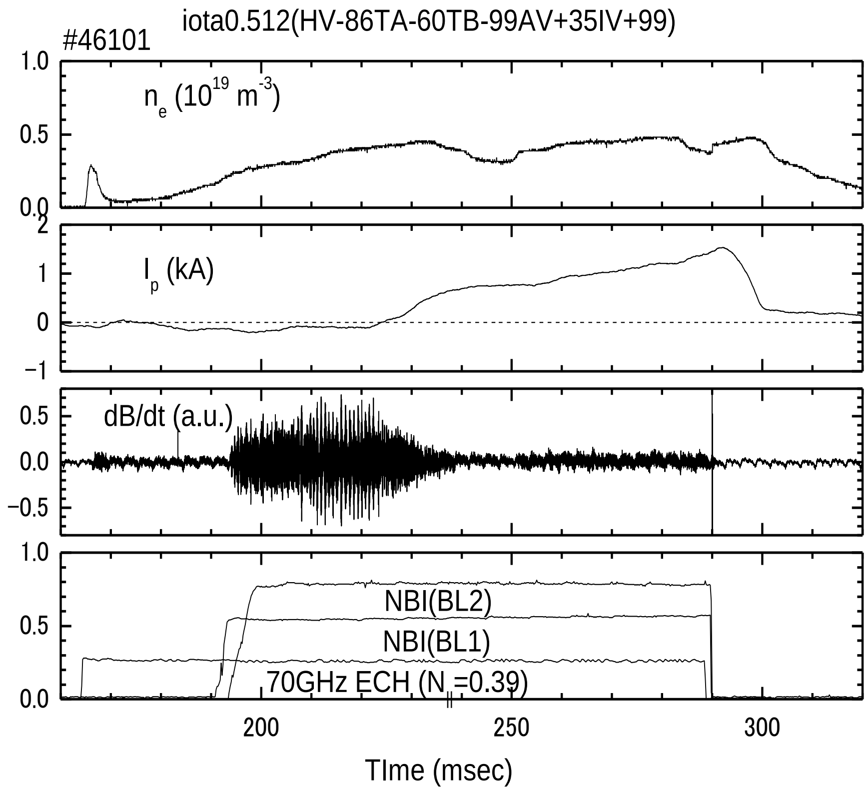

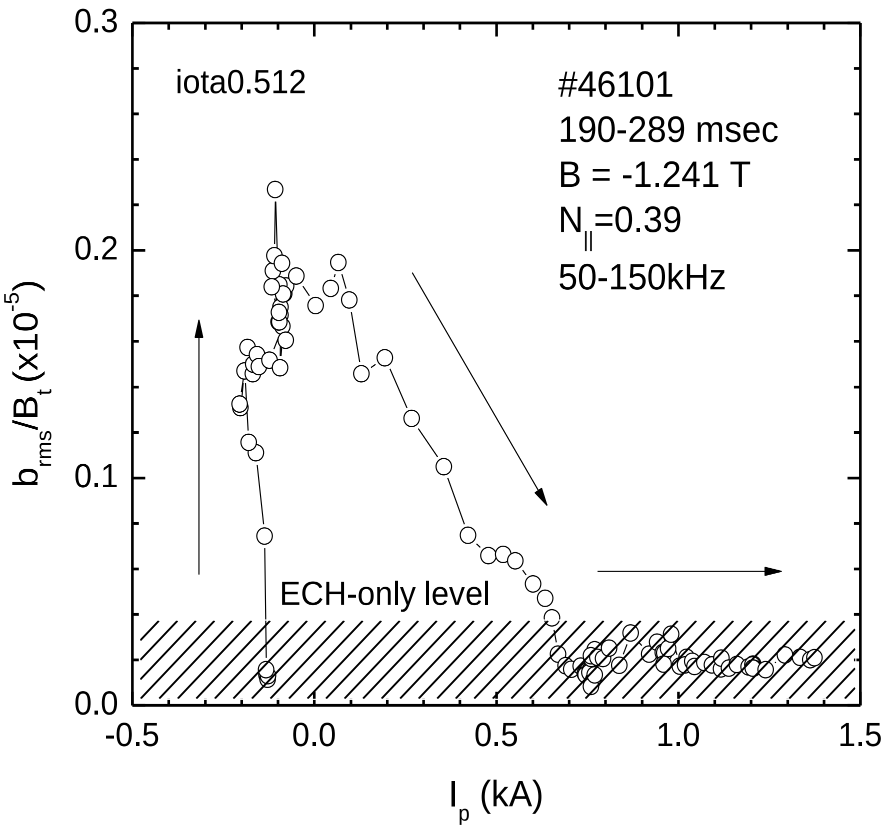

Co-ECCD is Also Effective for Stabilizing Energetic-Ion-Driven MHD Modes

No ECCD ($N_{||}$=0.0)

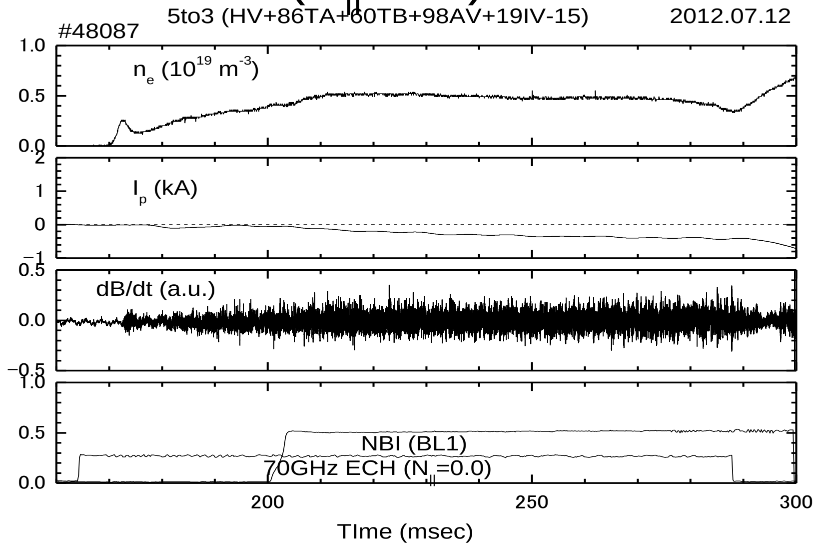

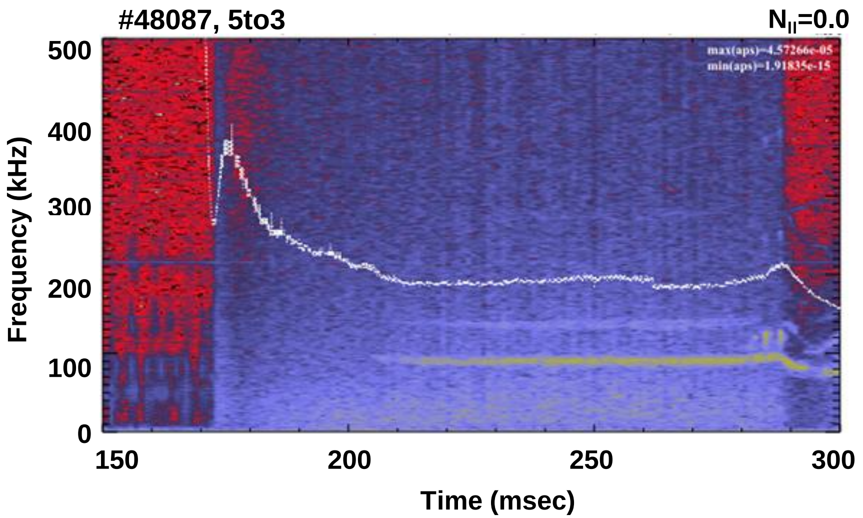

Co-ECCD ($N_{||}$= 0.4)

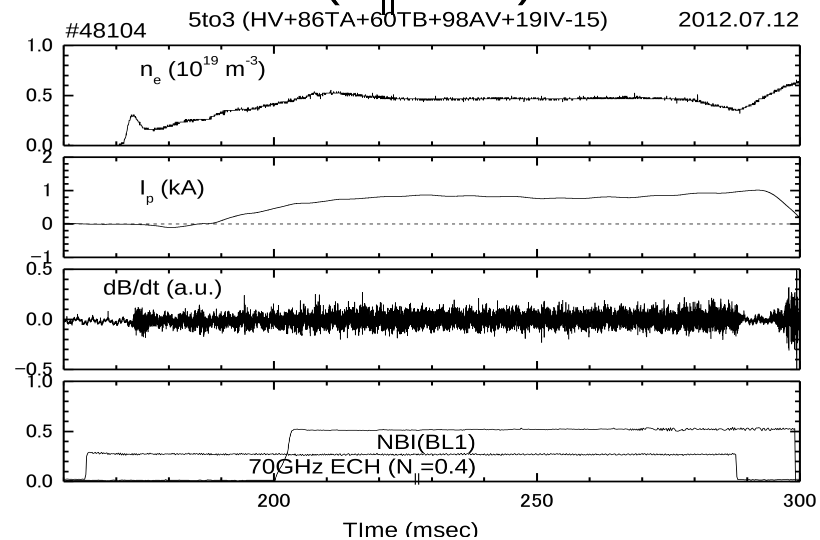

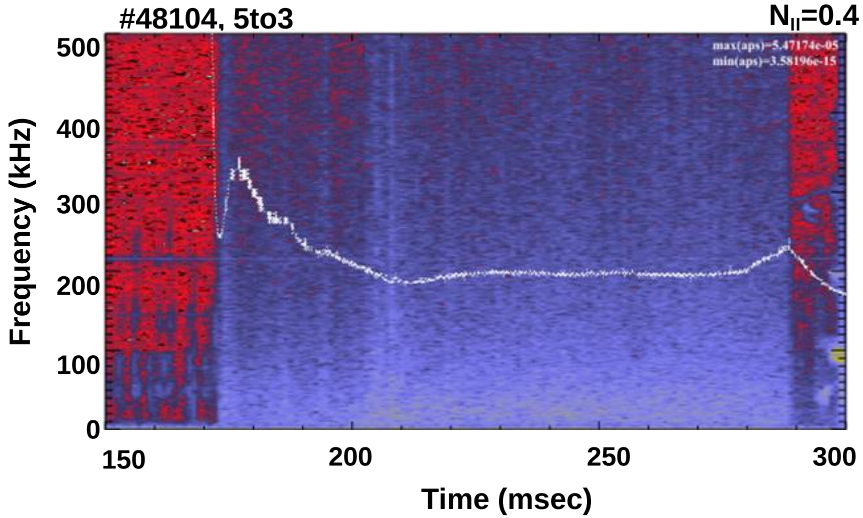

EPM Is Stabilized When Magnetic Shear Exceeds a Threshold Value

- For counter-ECCD, when the magnetic shear is larger than 0.12, the mode amplitude is completely suppressed to the level of ECH-only phase
- Similar suppression is observed for co-ECCD, but the threshold shear is not clear

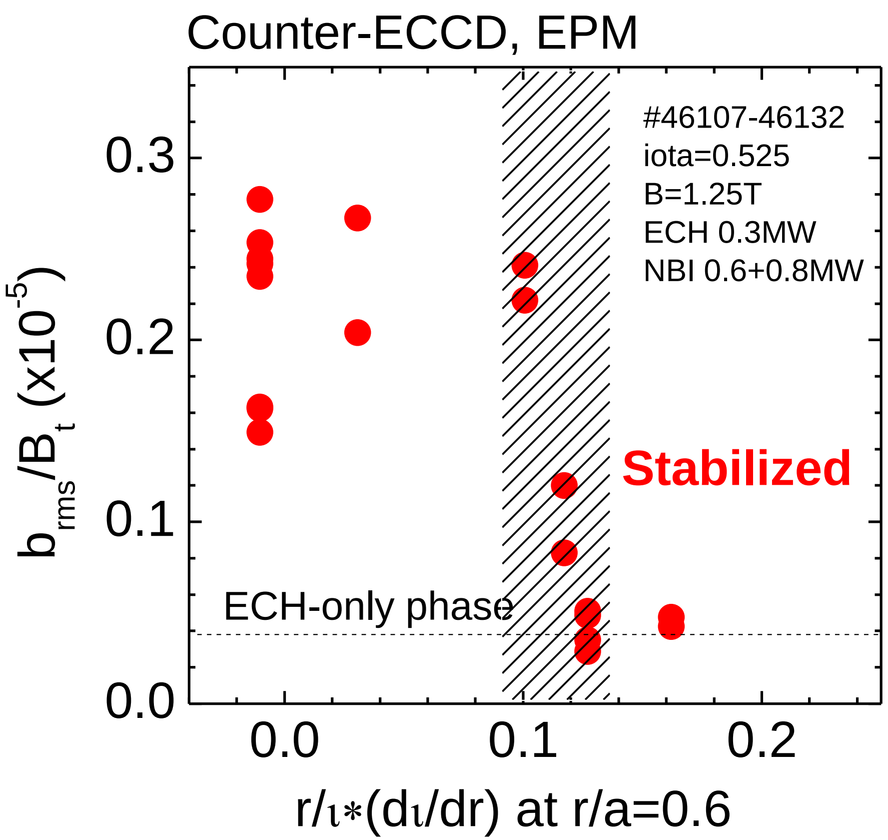

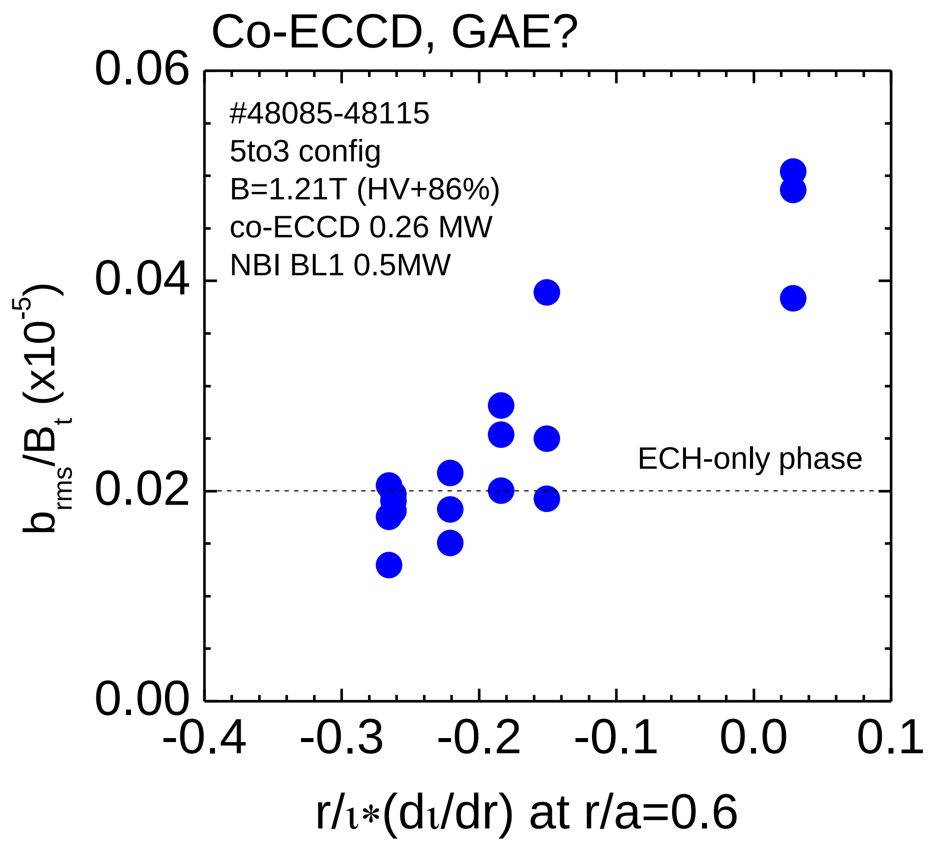

Stabilization Mechanism of EPM by ECCD

- EPM is mitigated by the change in magnetic shear due to ECCD where continuum damping is the main mechanism for stabilization

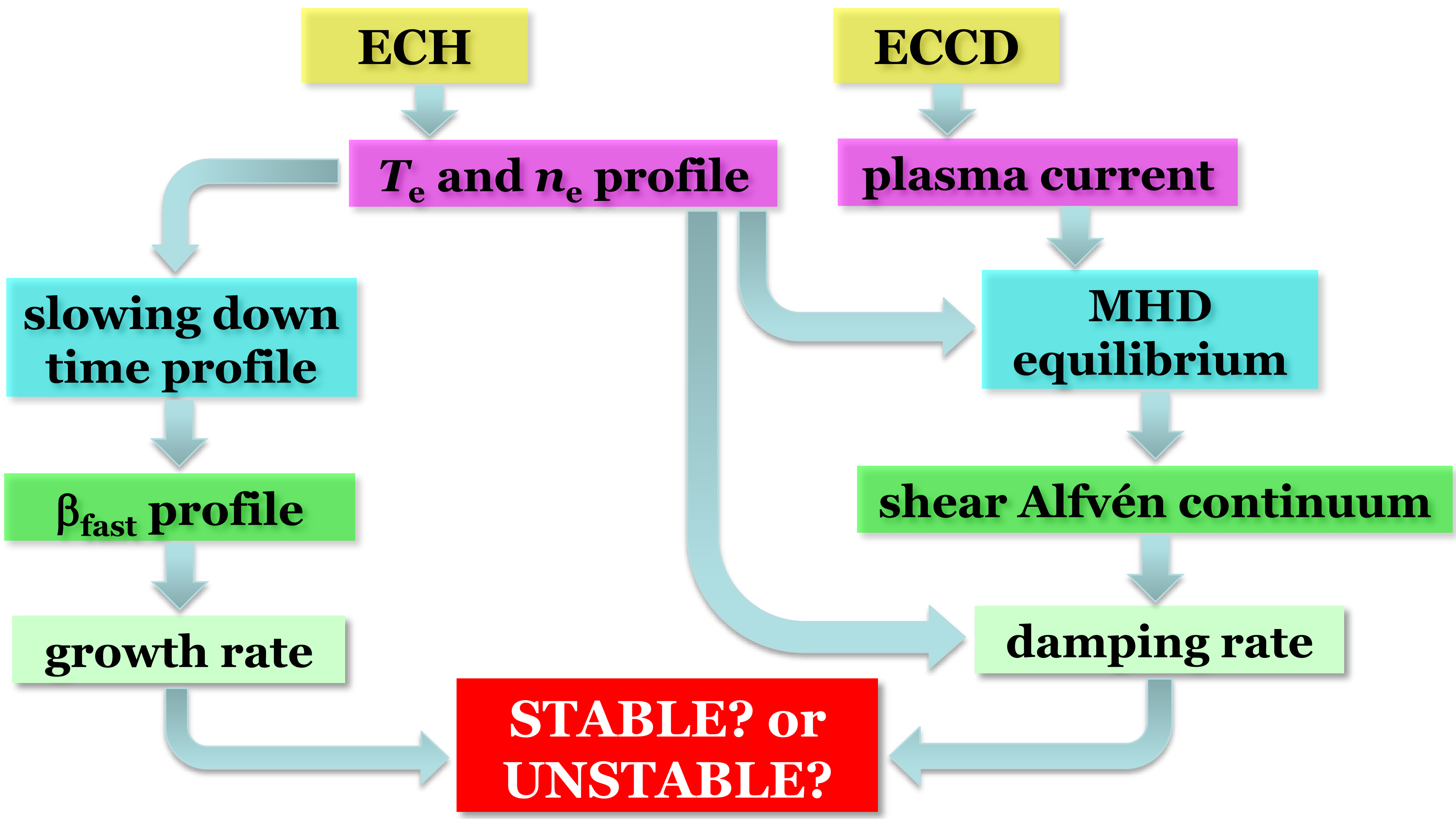

Conclusions

- Energetic-ion-driven MHD modes such as GAE and EPM are often observed in Heliotron J NBI plasmas
- An EC current of a few kA driven in the central region modifies the rotational transform profile from a shearless flat one into a high-shear one in the medium-sized stellarator/Heliotron device, Heliotron J
- The energetic-ion-driven MHD modes have been stabilized by centrally localized second harmonic 70-GHz X-mode ECCD
- Both co-ECCD (negative magnetic shear) and counter-ECCD (positive magnetic shear) are effective at stabilizing energetic-ion-driven MHD modes
- $N_{||}$ scan indicates that an EPM is stabilized when the positive (possibly negative also) magnetic shear exceeds a critical threshold
- Comparison with AE theory is required to clarify the stabilization mechanism

Plans in 2014: T_e Profile Measurement Using EBE

Collaboration with F. Volpe (Columbia Univ.)

- T_e profile measurement using EBE is under development under collaboration with Columbia Univ. and NIFS
- The cut-off density for O-mode is medium, n_e~$2x10^{19}m^{-3}$.
- Ray tracing calculation shows that an O-X mode conversion window is accessible
- A radiometer for 24-42GHz has been assembled and tested

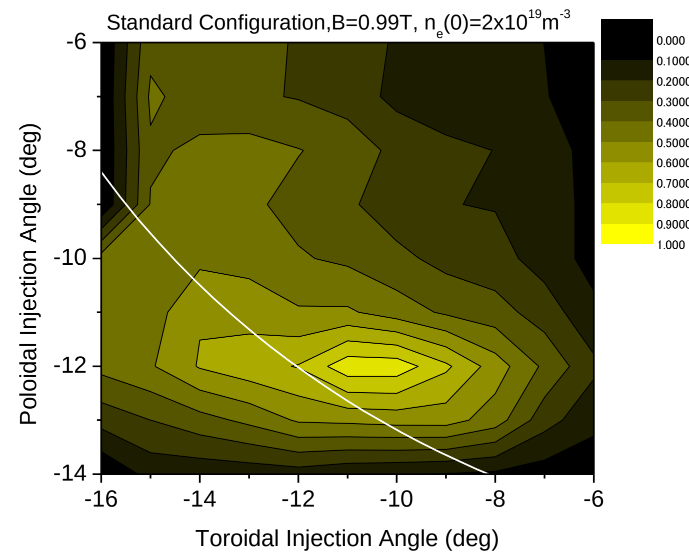

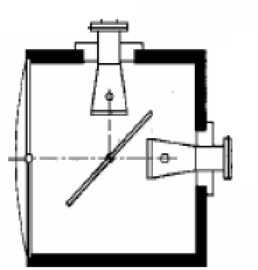

Gaussian Optics Antenna

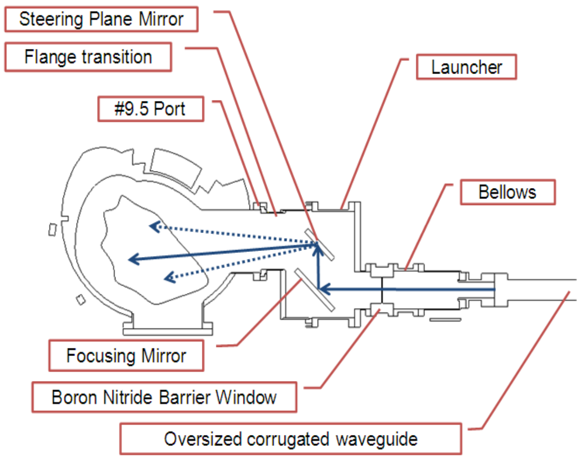

W. G. Switch

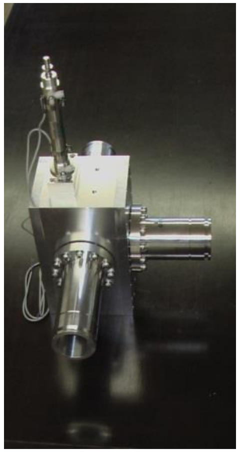

Induced Electric Field Affects Time Evolution of EC Driven Current

- The iota profile reaches quasi-steady state after 50 msec under the experimental condition, n_e=0.5×10^{19} m^{-3} and $T_e(0)$=0.8 keV

1-D current diffusion equation

$$\mu_0 \frac{\partial I_p}{\partial t} = 4\pi S \frac{\partial}{\partial S}\left\{\frac{1}{\sigma}\frac{\partial}{\partial S}\left(I_p - I_{NI}\right)\right\}$$

$I_p(S)$: total current
$I_{NI}(S)$: noninductive current
S: $S=\pi r^2$, σ: electrical conductivity

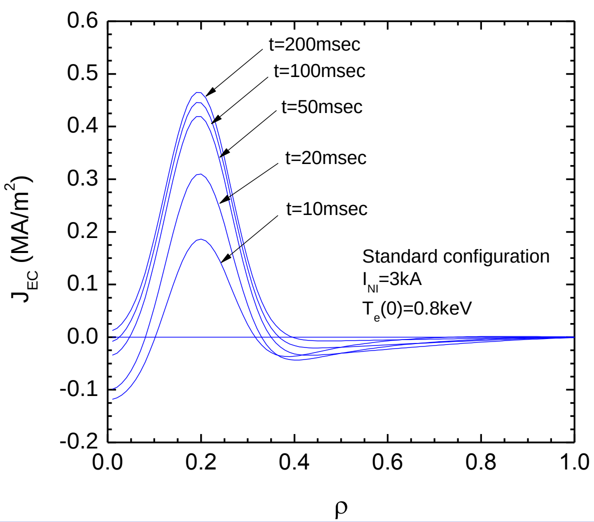

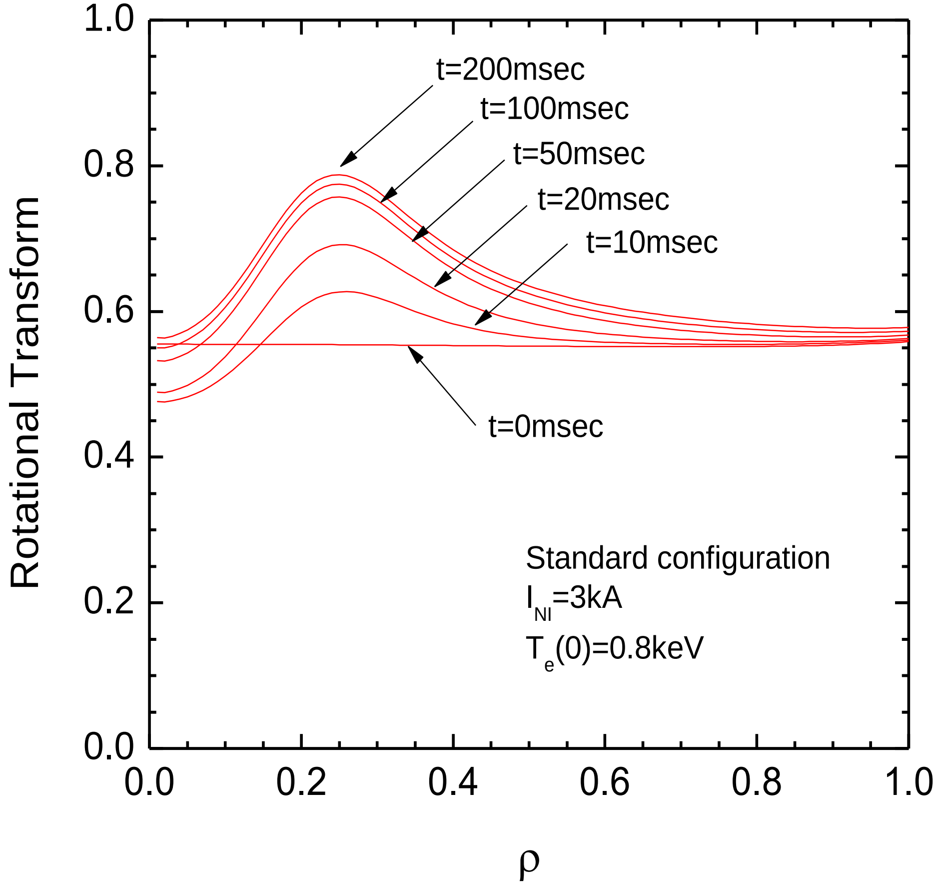

Adjoint Approach for ECCD Calculation

- current driven by RF source,

$$j_{\|} = -e\int \mathrm{d}u\ v_{\|}\ \delta f_e \quad \text{with} \quad \delta f_e = f_e - F_{eM} \quad \text{and} \quad u = \gamma v$$

can be calculated by solving DKE,

$$\frac{d\delta f_e}{dt} - C^{lin}(\delta f_e) = Q_{RF}(F_{eM}) \equiv -\frac{\partial}{\partial \mathbf{u}} \cdot \mathbf{\Gamma}_{RF}$$

- idea: exploiting the self-adjoint properties of $C^{lin}(\delta f_e)$ to express CD through the response function formally identical to the solution of (generalized) Spitzer-Härm problem (Hirshman, 1980; Antonsen & Chu, 1982; Taguchi, 1983)

  - If solution of the adjoint kinetic eq-n is known,

$$\frac{dg}{dt} + C^{lin}(g) = \nu_{e0}\frac{v_{\|}}{v_{th}} b F_{eM} \quad \text{with} \quad b = B/B_{\max},$$

then with $g(s;\ u,\xi) = \chi(s;\ u,\xi)F_{eM}(u)$ and $\xi = v_{\|}/v$

$$\langle j_{\|}\rangle = \frac{e v_{th}}{\nu_{e0}} \cdot \frac{\langle b\rangle}{\langle b^2\rangle} \cdot \left\langle \int d\mathbf{u}\ \frac{\partial \chi}{\partial \mathbf{u}} \cdot \mathbf{\Gamma}_{RF} \right\rangle$$

- Presently, adjoint approach is most common for ray- and beam-tracing